Introduction to Special Issue - In-depth study of air pollution sources and processes within Beijing and its surrounding region (APHH-Beijing)

Zongbo Shi[1,2 *], Tuan Vu[1], Simone Kotthaus[3,4], Roy M. Harrison[1†], Sue Grimmond[3], Siyao Yue[5], Tong Zhu[6], James Lee[7,8], Yiqun Han[6,9], Matthias Demuzere[10], Rachel E Dunmore[7], Lujie Ren[2,5], Di Liu[1], Yuanlin Wang[5,11], Oliver Wild[11], James Allan[12,13], Joe Acton[11], Janet Barlow[3], Benjamin Barratt[9], David Beddows[1], William J, Bloss[1], Giulia Calzolai[14], David Carruthers[15], David C Carslaw[7,16], Queenie Chan[9], Lia Chatzidiakou[17], Yang Chen[18], Leigh Crilley[1], Hugh Coe[12], Tie Dai[5], Ruth Doherty[19], Fengkui Duan[20], Pingqing Fu[2,5], Baozhu Ge[5], Maofa Ge[21], Daobo Guan[22], Jacqueline F. Hamilton[7], Kebin He[20], Mathew Heal[19], Dwayne Heard[23], C Nicholas Hewitt[11], Michael Hollaway[11], Min Hu[6], Dongsheng Ji[5], Xujiang Jiang[20], Rod Jones[17], Markus Kalberer[17,a], Frank J Kelly[9], Louisa Kramer[1], Ben Langford[24], Chun Lin[19], Alastair C Lewis[7], Jie Li[5], Weijun Li[25], Huan Liu[20], Junfeng Liu[26], Miranda Loh[27], Keding Lu[6], Franco Lucarelli[14], Graham Mann[28], Gordon McFiggans[12], Mark R. Miller[29], Graham Mills[30], Paul Monk[31], Eiko Nemitz[24], Fionna O'Connor[32], Bin Ouyang[11,17], Paul I. Palmer[19], Carl Percival[12,b], Olalekan Popoola[17], Claire Reeves[30], Andrew R Rickard[7,8], Longyi Shao[33], Guangyu Shi[5], Dominick Spracklen[28], David Stevenson[19], Yele Sun[5], Zhiwei Sun[34], Shu Tao[26], Shengrui Tong[21], Qingqing Wang[5], Wenhua Wang[33], Xinming Wang[35], Xuejun Wang[26], Zifang Wang[5], Liangfang Wei[5], Liangfang Wei[5], Lisa Whalley[23], Xuefang Wu[1], Zhijun Wu[6], Pinhua Xie[36], Fumo Yang[37], Qiang Zhang[38], Yanli Zhang[35], Yuanhang Zhang[6], Mei Zheng[6]

[1] School of Geography Earth and Environmental Sciences, the University of Birmingham, UK
[2] Institute of Surface-Earth System Science, Tianjin University, China
[3] Department of Meteorology, University of Reading, UK
[4] Institut Pierre Simon Laplace, Ecole Polytechnique, France
[5] Institute of Atmospheric Physics, Chinese Academy of Sciences, Beijing, China
[6] College of Environmental Sciences and Engineering, Peking University, Beijing, China
[7] Wolfson Atmospheric Chemistry Laboratories, Department of Chemistry, University of York, York, UK
[8] National Centre for Atmospheric Science, University of York, York, UK
[9] Analytical & Environmental Sciences Division, King's College London, London, UK
[10] Department of Geography, Ruhr-University Bochum, Bochum, Germany
[11] Lancaster Environment Centre, Lancaster University, Lancaster, UK
[12] School of Earth and Environmental Sciences, The University of Manchester, Manchester, UK
[13] National Centre for Atmospheric Science, The University of Manchester, Manchester, UK
[14] Dipartimento di Fisica e Astronomia, University of Florence, Florence, Italy
[15] Cambridge Environmental Research Consultants, Cambridge UK
[16] Ricardo Energy & Environment, Harwell, Oxfordshire
[17] Department of Chemistry, University of Cambridge, Cambridge, UK
[18] Chongqing Institute of Green and Intelligent Technology, Chinese Academy of Sciences, Chongqing, China
[19] School of Geosciences, University of Edinburgh, Edinburgh, UK
[20] School of Environment, Tsinghua University, Beijing China
[21] Institute of Chemistry, Chinese Academy of Sciences, Beijing, China
[22] School of International Development, University of East Anglia, Norwich, UK
[23] Department of Chemistry, University of Leeds, Leeds, UK
[24] Centre for Ecology & Hydrology, Penicuik, UK
[25] School of Earth Sciences, Zhejiang University, Hangzhou, China

[†] Also at: Department of Environmental Sciences / Center of Excellence in Environmental Studies, King Abdulaziz University, PO Box 80203, Jeddah, 21589, Saudi Arabia
[a] Now at: University of Basel, Department of Environmental Sciences, Klingelbergstrasse 27, 4056 Basel, Switzerland
[b] Now at Jet Propulsion Laboratory, 4800 Oak Grove Drive, Pasadena, CA 91109, USA

[26] College of Urban and Environmental Sciences, Peking University, Beijing, China
[27] Institute of Occupational Medicine (IOM), Edinburgh, UK
[28] School of Earth and Environment, University of Leeds, Leeds, UK
[29] Centre for Cardiovascular Science, Queen's Medical Research Institute, University of Edinburgh, Edinburgh, UK
[30] School of Environmental Studies, University of East Anglia, Norwich, UK.
[31] Department of Chemistry, University of Leicester, Leicester, UK
[32] Hadley Centre, Met Office, Reading, UK
[33] State Key Laboratory of Coal Resources and Safe Mining & College of Geosciences and Surveying Engineering, China University of Mining and Technology (Beijing)
[34] School of Public Health, Capital Medical University, Beijing, China
[35] Guangzhou Institute of Geochemistry, Chinese Academy of Sciences, Guangzhou, China
[36] Anhui Institute of Optics and Fine optics, Chinese Academy of Sciences, Hefei, China
[37] Department of Environmental Science and Engineering, College of Architecture and Environment, Sichun University, Chengdu, China
[38] Department of Earth System Science, Tsinghua University, Beijing, China

[*] *Corresponding to*: Zongbo Shi (email: z.shi@bham.ac.uk)

Abstract. The Atmospheric Pollution and Human Health in a Chinese Megacity (APHH-Beijing) programme is an international collaborative project focusing on understanding the sources, processes and health effects of air pollution in the Beijing megacity. APHH-Beijing brings together leading China and UK research groups, state-of-the-art infrastructure and air quality models to work on four research themes: (1) sources and emissions of air pollutants; (2) atmospheric processes affecting urban air pollution; (3) air pollution exposure and health impacts; and (4) interventions and solutions. Themes 1 and 2 are closely integrated and support Theme 3, while Themes 1-3 provide scientific data for Theme 4 to develop cost-effective air pollution mitigation solutions. This paper provides an introduction to (i) the rationale of the APHH-Beijing programme, and (ii) the measurement and modelling activities performed as part of it. In addition, this paper introduces the meteorology and air quality conditions during two joint intensive field campaigns - a core integration activity in APHH-Beijing. The coordinated campaigns provided observations of the atmospheric chemistry and physics at two sites: (i) the Institute of Atmospheric Physics in central Beijing, and (ii) Pinggu in rural Beijing during 10 November – 10 December 2016 (winter) and 21 May- 22 June 2017 (summer). The campaigns were complemented by numerical modelling and automatic air quality and low-cost sensor observations in the Beijing megacity. In summary, the paper provides background information on the APHH-Beijing programme, and sets the scene for more focussed papers addressing specific aspects, processes and effects of air pollution in Beijing.

1. Introduction

Air pollution is one of the largest environmental risks. It is estimated that air pollution has led to 7 million premature deaths per year globally (WHO, 2016a, b) and over a million in China (GBD MAPS

Working Group, 2016). Air pollution also has significant impact on the healthcare system and ecosystems, which cost about 0.3% of global GDP (OECD, 2016). Air pollution related sickness also reduces productivity and severe hazes lead to closure of transport systems, causing additional damage to the economy. Total economic losses related to China's $PM_{2.5}$ (particulate matter with aerodynamic diameter equal to or less than 2.5 µm) pollution in 2007 amounted to 346 billion Yuan (£39 billion, approximately 1.1% of the national GDP) based on the number of affected Chinese employees whose work time in years was reduced because of mortality, hospital admissions and outpatient visits (Xia et al., 2016).

Considerable research effort has led to huge progress in understanding the sources and pollution processes in megacities in western countries, e.g., major interdisciplinary and multi-institutional programmes in Paris and London in the last few years (Beekmann et al., 2015; Bohnenstengel et al., 2014). Although air pollution in developed megacities sometimes breaks country specific limits and WHO guidelines, traditional London or Los Angeles type smogs which occurred in the early and mid-20th centuries are rare in developing cities to the same extent. In the developing countries however, the rush to industrialisation and rapid growth in vehicle populations have led to serious air pollution problems that are more complex than the London or Los Angeles smogs.

Air pollution is particularly severe in developing megacities, such as Beijing, where pollutants from traditional sources, such as solid fuel combustion are mixed with those from modern vehicles (Guan et al., 2014), on top of regional pollution from industrial and other anthropogenic activities. Air pollution in Beijing is different to that in well studied developed megacities, such as Paris and London, in a number of ways including the lack of diesel emissions in the inner city, the use of coal in surrounding rural areas for heating and domestic cooking (Tao et al., 2018), the high emissions of air pollutants in neighbouring provinces (Hebei and Tianjin) and the high oxidising power due to the complex chemistry (Zhang et al., 2009; Li et al., 2017; Lu et al., 2018). This makes Beijing a particularly interesting place to study as it provides an atmospheric environment with major contrasts to developed megacities such as London and Paris in which to investigate urban pollution processes.

Many research programmes have been initiated in Beijing to study the air pollution processes since the late 1990s. Earlier research programmes (e.g., early 2000) focused on primary emissions of SO_2, NO_2, CO, PM_{10}, volatile organic compounds, and subsequently secondary pollutants such as ground-level ozone and secondary fine particles. This research contributed to the development of air pollution mitigation strategies introduced by the Beijing Municipal government.

The Beijing Olympic Games (2008) offered additional incentives to improve air quality and this led to the funding of CAREBEIJING (Campaigns of Air Pollution Research in Megacity Beijing and Surrounding Region) and other major programmes. The field campaigns were conducted in the summer of 2006, 2007, and 2008, with the objectives to learn the environmental conditions of the region, to identify and quantify the processes (transport and transformation) that led to the impact of the surrounding area on air quality in Beijing, and to formulate policy suggestions for air quality improvement during the 2008 Beijing Olympic Games. Measures developed as a result of this and other programmes successfully improved air quality during the Olympics Games, and provided valuable examples for developing air pollution control policy in other cities (Wang et al., 2010). CARE-BEIJING was later extended to CAREBEIJING-NCP (Campaigns of Air Pollution Research in Megacity Beijing and North China Plain), in which field campaigns were carried out in the summer of 2013 and 2014 to investigate the transport and transformation processes of air pollutants in the Beijing megacity and North China Plain. The results of CAREBEIJING and CAREBEIJING-NCP have been published in three special issues of Atmospheric Chemistry and Physics (https://www.atmos-chem-phys.net/special_issue198.html) and Journal of Geophysical Research-Atmospheres (https://agupubs.onlinelibrary.wiley.com/doi/toc/10.1002/(ISSN)2169-8996.CARBS1). However, our understanding of sources and emissions of key air pollutants such as $PM_{2.5}$ and ozone and the role of the interactions between physical and chemical processes in the development of pollution events in Beijing is still far from being accurate or complete. In addition, none of the abovementioned large programmes have been directly linked to health effect studies.

The adverse health effects of air pollution provide one of the key motivations to control air pollution. Research has shown that air pollution is one of the leading causes of the disease burden in China (GBD MAPS Working Group, 2016). Especially, particulate pollution, the leading cause of severe air pollution events in China, has a significant impact on human health and is associated with high mortality (Zhang et al., 2017a), with a considerable proportion of this related to cardiorespiratory diseases (namely stroke, ischemic heart disease, and chronic obstructive pulmonary disease) (Yang et al., 2013; Lozano et al., 2013). Despite this increasing evidence base, the adverse health impact of air pollution remains a complex issue. For instance, the risk assessment of disease burden due to air pollution in China has relied largely on the studies undertaken in Europe and North America, which may be subject to error due to the difference of race, life style, and air pollution settings (Lim et al., 2012). The marked change in air pollution sources and composition between the heating and non-heating seasons, and the differences between urban and rural areas may all lead to different biological responses in local populations. However, to date, such comparative investigations are largely lacking. A further limitation of such work is the lack of accurate personal exposure estimates which are crucial in high quality health studies. This may be

especially true when considering household air pollution (both indoors and outdoors) from traditional biomass and coal stoves which may not be easily captured by typical outdoor monitoring instruments (Linn et al., 2001; Brook et al., 2002). Thus, understanding the health impact of air pollution in China remains a major challenge.

To address these issues, the UK Natural Environment Research Council (NERC), in partnership with the National Science Foundation of China (NSFC), UK Medical Research Council (MRC) and UK-China Innovation Newton Fund funded a major joint research programme – Atmospheric Pollution and Human Health in a Chinese Megacity (APHH-Beijing). The APHH-Beijing is an integrated research programme, incorporating the capabilities and strengths of the UK and Chinese science communities which is taking a multi-disciplinary approach to investigating the sources, processes and health effects of air pollution in the Beijing megacity. The new scientific understanding underpins the development of interventions and solutions to improve air quality and reduce health impacts.

This special issue "In-depth study of air pollution sources and processes within Beijing and its surrounding region (APHH-Beijing)" documents the research outcomes of this APHH-Beijing programme, in particular the atmospheric measurement and modelling aspects.

This introduction paper describes the motivation and background of the APHH-Beijing programme, and presents some of the background air quality and meteorological observations, particularly during the two intensive field campaigns. These campaigns form one of the core research activities within APHH-Beijing integrating the different themes / projects. We do not present the key scientific results of APHH-Beijing in this introduction (not an overview) paper as much of the research activity are still ongoing and unpublished. Key findings will be published in the Special Issue to which this paper provides key background information.

2. APHH-Beijing Programme Objectives

The overall aim of APHH-Beijing is to better understand the sources, atmospheric transformations and health impacts of air pollutants in the Beijing megacity and to improve the capability of forecasting air quality and developing cost-effective mitigation measures. Specific objectives include:

- to determine the emission fluxes of key air pollutants and to measure the contributions of different sources, economic sectors and regional transport to air pollution in Beijing
- to improve understanding of the processes by which pollutants are transformed or removed through transport, chemical reactions and photolysis and the rates of formation and conversion of particulate matter (PM) via atmospheric reactions

- to improve understanding on how the detailed properties of PM evolve and can influence their physical properties and behaviour in the atmosphere and elucidate the mechanisms whereby those properties may interact and feedback on urban scale and regional meteorology
- to exploit new satellite observations and regional models to place the *in-situ* campaigns into a wider context
- to determine the exposure of Beijing inhabitants to key health related pollutants using personal air pollution monitors and assess the association between air pollution exposure and key cardiopulmonary measures
- to determine the contribution of specific activities, environments and pollution sources to the personal exposure of the Beijing population to air pollutants
- to enhance our understanding of the health effects in susceptible individuals over time periods when there are large fluctuations in pollutants compared with normal controls, and to identify health outcomes of air pollution
- to estimate economic loss due to both physical and mental impacts of air pollution and examine how Beijing can improve its air quality more cost effectively

3. Research Themes and Integration within the APHH-Beijing Programme

The APHH-Beijing programme has four themes to address the specific objectives outlined in Section 2, and is delivered through five inter-related research projects:

- Theme 1 - Sources and emissions: delivered by the AIRPOLL-Beijing (Source and Emissions of Air Pollutants in Beijing) project;
- Theme 2 – Atmospheric processes: delivered by the AIRPRO (The integrated Study of AIR Pollution PROcesses in Beijing) project;
- Theme 3 – Health effects: delivered by two projects - the AIRLESS (Effects of AIR pollution on cardiopuLmonary disEaSe in urban and peri-urban reSidents in Beijing) and the APIC-ESTEE (Air Pollution Impacts on Cardiopulmonary Disease in Beijing: An integrated study of Exposure Science, Toxicogenomics and Environmental Epidemiology) projects;
- Theme 4: Solutions: delivered by the INHANCE (Integrated assessment of the emission-health-socioeconomics nexus and air pollution mitigation solutions and interventions in Beijing) project.

3.1 Research Themes

3.1.1 Theme 1: Sources and emissions

AIRPOLL aims to quantify the emission fluxes of key air pollutants in Beijing and the contributions of different sources, economic sectors and regional transport to air pollution in Beijing. The project has

carried out two major field observation campaigns jointly with the AIRPRO and AIRLESS projects (Sections 3.1.2 and 3.1.3) during November-December 2016 and May-June 2017. The campaigns were carried out at two sites - one within Beijing (at the Institute of Atmospheric Physics (IAP) meteorological tower site) and the other in the local region (the rural Pinggu site – see 4.1 for site information).

During the intensive campaigns, the project measured the fluxes of particulate and gaseous air pollutants from ground-level sources by sampling on the meteorological tower (325 m) at the IAP site, which are being compared with emissions estimates taken from the inventory for Beijing. This was complemented by top-down fluxes inferred from satellite data for nitrogen dioxide, sulphur dioxide and formaldehyde, the latter indicative of VOC oxidation processes (Palmer et al., 2003; Fu et al., 2007). Through these means, the emissions inventory is being tested, allowing revisions which are being incorporated into the atmospheric modelling work.

AIRPOLL also made very detailed on-line and off-line measurements of airborne particles. This included continuous measurements of size distributions from 1 nm to >10 µm diameter. Large molecules and molecular clusters were also measured by high resolution mass spectrometry, with a view to better understanding atmospheric nucleation processes. The project has monitored the chemical composition of particles in real time by Aerosol Mass Spectrometry and analysed the time-integrated particle samples off-line for major and minor constituents, including organic molecular markers. AIRPOLL determined the carbon-14 in water soluble organic carbon, water insoluble organic carbon and elemental carbon in selected time-integrated particle samples with an aim to differentiate fossil and non-fossil particulate carbon. These data are being brought together for use in receptor modelling of PM sources, which are compared with other estimates of source contributions to PM concentrations. Measured ground-level concentrations both from our campaign sites and the Beijing monitoring network, together with vertical gradient observations at the tower and source apportionment results are compared with the predictions of a chemistry-transport model and used to provide a clear distinction between advected regional pollution and the impact of local sources. Divergences between measured and modelled pollutant concentrations will be used to provide critical evaluation of emissions inventories, which will be enhanced iteratively with a view to improving knowledge of the sources and emissions of pollutants affecting air quality in Beijing.

During the campaigns, AIRPOLL and AIRLESS measured the concentrations of key tracers and reactive species indicative of sources and chemical pathways at the ground-level sites, which complements AIRPOLL observations.

3.1.2 Theme 2: Atmospheric processes

AIRPRO aims to study the fundamental chemical and physical processes controlling gas and particle pollution, localised meteorological dynamics, and the links between them within Beijing's atmosphere. Central to the project were the intensive *in situ* measurements at the IAP meteorological tower (325 m) site, jointly carried out with the AIRPOLL project. AIRPRO made comprehensive and detailed local observations of both primary emitted chemicals and particles, radical intermediates and secondary products, for periods of contrasting local and regional emissions, solar insolation and air temperature. These data allow the performance of local and regional models of air pollution to be robustly tested, both for final regulated pollutant outcomes and at a more mechanistic level.

Observations made with instruments from multiple Chinese and UK research groups included complementary measurements of key precursor trace gases such as NO_x, HONO, SO_2, CO, O_3, VOCs and SVOCs, gas phase radicals such as OH, HO_2, RO_2, and NO_3, and PM including chemical (both on-line and offline analyses), biological, physical and optical properties. Through multiple co-located surface measurements, there was both instrumental redundancy (e.g. for equipment failures) and capacity to evaluate through inter-comparison some hard-to-measure atmospheric free radicals and gases such as OH, HO_2, N_2O_5, HCHO and other oxygenated VOCs. The project determined the local *in situ* chemical processing of air pollution in the contrasting winter/summertime periods alongside overall atmospheric reactivity, both day and at night, through a combination of modelling and proxy measurements such as measured ozone production efficiency and OH reactivity.

The IAP tower allowed vertical profiles of key pollutants up to 320 m to be obtained and, with additional remote sensing of composition and meteorology, provided insight into boundary layer stability and evolution over the diurnal cycle. Quantification of shallow mixed layers proved to be vital for explaining local surface *in situ* chemical processing and also street level concentrations of relevance to exposure. The potentially significant vertical gradients anticipated in some chemicals and PM properties were further quantified using instruments installed on the tall tower and via profiling gondola measurements. The combined datasets, surface and profiles, provide the basis for evaluation of model performance, and notably comparisons for those intermediates that provide indicators of whether secondary pollution production is being correctly simulated.

3.1.3 Theme 3: Health effects

Health effects of air pollution are studied by two projects – AIRLESS and APIC-ESTEE. AIRLESS aims to advance air quality and health research in Beijing by bringing together two fields of research that have made rapid advancements in recent years: measurements of a wide range of pulmonary and cardiovascular biomarkers in a panel study and personal monitoring of multiple air pollutants with high spatio-temporal resolution by sensor technology. AIRLESS is also benefiting from the use of an extensive range of

pollution metrics and source apportionment results from the AIRPOLL and AIRPRO projects. These data are being compared with our personal air quality assessments and used to further understanding of the nature of the air pollution exposures of residents and how this relates to their health status.

APIC-ESTEE aims to evaluate the impacts of air pollution on cardiopulmonary health through an integrated study of exposure, epidemiology, and toxicology/toxicogenomics. APIC-ESTEE has investigated the relationship between ambient air pollution and personal exposures. This is being used to estimate personal exposures for epidemiological analyses of long term health impacts in a cohort study and of short-term effects (i.e. biomarkers, blood pressure, heart rhythm, and peak flow) in a panel study. APIC-ESTEE also studied the real-world exposure-reduction and health benefit potential of face-masks, a commonly used personal level intervention seen in Beijing. Furthermore, to complement the human based studies into mechanisms of action, APIC-ESTEE has conducted *in vivo* analyses of mechanistic effects and early life toxicogenomics/metabonomics.

3.1.4 Theme 4: Solutions

INHANCE aims to quantitatively evaluate the performance of China's current air pollution policies and develop cost-effective solutions to mitigate the impact of air pollution in the Beijing megacity. INHANCE considered not only the physical and mental health impacts and direct economic impact, but also the cascading indirect economic losses occurred through inter-industrial and inter-regional linkages on the supply side of the economy. INHANCE has established and evaluated interactive relationships among exposure, vulnerability, impact on health, implications for industry and economic consequences. INHANCE has compared and qualitatively assessed air quality policies between Beijing and other cities, undertaken policy performance assessment modelling, utilised techno-economic inventories for anti-pollution measures to conduct micro cost-benefit analysis of new policies; measured health and macroeconomic costs and benefits in mitigating air pollution, and, transformed evidence generated into practical emission alleviation pathways. On these bases, INHANCE will deliver recommendations regarding integrated policy design and an assessment for policy cost-effectiveness.

3.2 Integration Between the Themes and Novelty of the APHH-Beijing Programme

The APHH-Beijing programme is highly integrated to ensure the biggest possible scientific and policy impacts. One of the most significant integration activities between the different themes is the coordinated joint field campaigns at an urban and a rural site in Beijing for Theme 1, 2 and 3 to fully exploit the complementary measurements and expertise by different research groups, which is described in the following sections. Theme 1 and 2 are closely related and in many senses inseparable. For example, our knowledge of the sources and emissions is essential to interpret the processes while knowledge on the atmospheric physical and chemical processes will help us to more accurately quantify the source emissions, both via actual flux-based measurements and model evaluation of the emission inventories.

Furthermore, to ensure integration, Themes 1 and 2 co-located their rural site at Pinggu as that was selected for the Theme 3 panel study.

Modelling of airborne concentrations of air pollutants within Themes 1 and 2 is fully integrated, primarily via the UKCA (UK Chemistry and Aerosol), NAQPMS (Nested Air Quality Prediction Model System) and GEOS-Chem models. The models simulate spatial and temporal variations of key air pollutants and are being evaluated using the new observations of pollutant emission fluxes, updated emission inventories, three-dimensional air quality low cost sensor observations, comprehensive composition and physics measurements, as well as new process understandings generated from the APHH-Beijing programme. Furthermore, in Themes 1 and 2, ADMS (Atmospheric Dispersion Modelling System) modelling results for the campaign periods facilitate the estimation of population exposure in Theme 3. Outcomes of Themes 1, 2 and 3 help to provide Theme 4 with a more accurate estimate of pollution costs and to develop cost-effective air pollution control measures in Beijing.

The third stream of integration activities involves regular APHH-Beijing programme science and stakeholder engagement meetings to stimulate collaboration and knowledge transfer between different themes and stakeholders. Furthermore, sharing of data was made available via a dedicated depository in Centre for Environmental Data Analysis (www.ceda.ac.uk). All data in the depository will be made publically available by the end of 2022.

Together, this interdisciplinary APHH-Beijing programme delivers key scientific values and innovation, including:

(1) Validation of the bottom-up emission inventories by using novel eddy covariance emission flux observations from the IAP meteorological tower, integrated with satellite retrievals and numerical modelling,

(2) Improvement in understanding of air pollution processes through comprehensive observations of atmospheric gaseous and aerosol species integrated with atmospheric physics measurements, and

(3) Identification of the sources of air pollution that cause largest adverse human health effects by carrying out novel cardiovascular health indicator measurements, integrated with personal exposure, fixed station source apportionment studies and high resolution air quality modelling.

4. Overview of the Joint Field Campaigns

The two intensive campaigns took place from 10th November to 10th December 2016 and 20th May to 22nd June 2017. The campaigns were carried out at both urban and rural sites.

4.1 Site Information

The winter campaign had two main sites. The urban site (39.97N, 116.38 E) is located in the Tower Section of the Institute of Atmospheric Physics (IAP), Chinese Academy of Sciences where the 325 m meteorological tower is located. The site, between the fourth and third North ring roads of Beijing (Figure 1), is in a residential area. Typical of central Beijing, there are various roads nearby. To the south, north and west there are roads about 150 m away. On site there are 2 to 3 floor buildings to the south, and the east and west of the tower surrounded by small trees and grass. There is a canal right to the north of the site. Further to the west is a park covered mainly by conifer pine trees (Yuan Dynasty Wall Heritage Park).

The rural Pinggu site in Xibaidian village (40.17N, 117.05 E) in north-eastern Beijing, was collocated with the AIRLESS project cohort. Xibaidian village is about 4 km northwest of Pinggu town centre, and about 60 km from IAP. There are several similar small villages nearby. The monitoring station and the clinic used an unoccupied house at the north end of the village away from significant local combustion sources. A two-lane road is about 300 m north of the site. With no centralised heating infrastructure available, residents mainly use coal and biomass for heating and cooking in individual homes.

In the summer, an additional site was operated in Gucheng (39.2N 115.7E), Dingxing County, Hebei Province. This site, about 120 km to the southwest of central Beijing, is on one of the main high pollutant transport pathways from Hebei province to Beijing from the southwest. The site is in a meteorological observatory surrounded by farm fields. The nearest town is about 10 km to the northeast. The nearest road is 500 m to the north and the nearest village ~1 km to the west. Several villages are located around the site.

In addition to the two highly instrumented urban (IAP) and rural (Pinggu) sites, 21 SNAQ (Sensor Network for Air Quality) boxes, which measure CO, NO, NO_2, CO_2, O_X, size resolved particulates (0.38-17.4 µm), temperature, relative humidity, wind speed and direction (Popoola et al., 2018), were deployed during the summer and winter campaigns across the urban and rural areas of Beijing to map air pollutant variations (red tags, Figure 1). Six additional SNAQ boxes were deployed at six different heights (8, 32, 102, 160, 260, and 320 m) on the IAP tower from 9-23 November 2016 and 25 January-31 December 2017.

Figure 1 also shows the location of the 12 national air quality monitoring stations. Hourly data for criteria air pollutants ($PM_{2.5}$, PM_{10}, SO_2, NO_2, CO and O_3) from January 2013 to December 2017 from the stations were also obtained from official sources. The closest air quality station to the urban IAP site is about 3 km away at the Olympic Park (G11, Figure 1).

4.2 Instrumentation

4.2.1 Urban site

Table 1 lists all instruments deployed during the campaigns at the IAP site. Most instruments ran during both campaigns. A majority of the instruments were situated in the nine containers, which were at ground level on the campus grass. A number of online instruments and high volume PM samplers were also deployed at different heights on the meteorological tower. Vertical profile measurements of atmospheric species including HONO were made during pollution events using baskets attached to the tower. Additional online measurements and offline PM samplers were deployed at ground-level, on the roof of a two storey building to the west (WB) and in a third-floor laboratory at the south end of the campus. In addition, high-, medium- and low-volume PM samplers were placed on the roof of WB for offline characterization and source apportionment.

4.2.2 Rural sites

At Pinggu, online instruments (Table 2) were run within an air-conditioned room on the ground floor with inlets on top of the building. High-, medium- and low-volume PM samplers were deployed on a newly modified flat-roof of the single storey building.

At Gucheng (summer only), a high volume Digitel sampler and a single particle sampler were set up on a deserted basketball court. An Aethalometer AE33 was located on top of a container at the edge of the basketball court. CO and O_3 were also measured in a nearby container.

4.3 Synoptic Scale Meteorology During the Field Campaigns

Synoptic circulation patterns (e.g., horizontal advection and wet deposition) play a key role in the variations of air quality in Beijing (Miao et al., 2017; Wu et al., 2017; Zhang et al., 2012). To provide the synoptic context of the APHH-Beijing observations, the daily mesoscale flow patterns have been classified and put into context using a 30-year climatology (Section 5.4).

Circulation types (CT) are classified using the software produced by the COST Action 733 “Harmonisation and Applications of Weather Type Classifications for European regions” (Philipp et al., 2010) with (ECMWF Re-Analysis) ERA-Interim 6-h 925 hPa geopotential reanalysis data (Dee et al., 2011) at its native 0.75° spatial resolution for the domain of interest (103-129° E, 31 - 49° N) centred on Beijing (40° N, 116.5° E) covering the period 1988-2017. ERA-Interim 10 m U and V wind components are used to facilitate the interpretation of the flow patterns. Of the COST733 methods (Huth et al., 2008; Philipp et al., 2010, 2016; Tveito and Huth, 2016) two are used: T-Mode PCA (Principal Component Analysis) and SANDRA (Simulated Annealing And Diversified RAndomization clustering). The former

have been used in Beijing previously (e.g. Miao et al., 2017; Zhang et al., 2012). The latter is considered to perform well in clustering pressure fields and discriminating environmental variables (e.g. Demuzere et al., 2011; Philipp et al., 2016). Classification is performed with the number of CTs ranging from 7 to 18. 11 CTs from the SANDRA method are selected (Figure 2; Table 3) to adequately represent the general flow conditions around Beijing during the 30 y climatology period (Beck and Philipp, 2010).

As expected, the CTs that occurred during the two field campaign periods are different (Figure 3). During the winter field campaign, the most frequent circulation type was CT 11 (24 % of the 6 h periods) which was often preceded by a period of CT 9 (total 13%). Circulation types 9-11 are associated with air masses that may stagnate over the Beijing urban area (Figure 2). CT 1 (accounting for 12% of the time) and CT 2 (17 %) are associated with the Asian winter monsoon which brings cold and dry air masses to eastern China. North-westerly flow (over Beijing) is driven by high pressure in the west of the domain (Figure 2), which are followed by CTs 5, 3 and 7 occurred 14, 7, and 5% of the time, respectively. CTs 3 and 5 are associated with relatively low pressure in the northeast (Sep-May period) while CT 7 has a south-easterly winds from the Bohai Sea. CTs 4, 6 and 8 did not or hardly occur during the winter campaign.

During the summer campaign (Figure 3b), the most frequent CTs were 8, 7, 4, and 6 (23, 25, 19, and 10 % of the time, respectively). CTs 8 and 6, which did not occur during the winter campaign period, are associated with the summer monsoon advecting moist, warm air from the South and Southeast (Figure 2). While southerly and northerly flows converge over Beijing for CT 6, slightly weaker low pressure to the Northeast means North-westerly flow dominates for CT 4. High pressure to the West or South of Beijing is rare during the summer campaign so that CTs 1, 2, 9, and 11 do not occur and CTs 3 and 5 are rather rare (6 and 1%, respectively).

4.4 Meteorological Conditions During the Field Campaigns

To assess how local-scale flow related to ERA-Interim fields (Section 4.3) compared to local conditions, the link between the coarse gridded data and tower-based sonic anemometer observations are explored based on wind roses (Figure 4). The 30 y climatology (Figure 4a, d) confirms the clear seasonality in wind direction affecting the occurrence of CTs discussed (Sect. 4.3), i.e. during winter intensive campaign period (10 November – 10 December) north-easterly flow clearly dominates while southerly wind directions are most common during the summer campaign period (20 May – 22 June). The wind roses for winter 2016 and summer 2017 (Figure 4b, e) are slightly nosier, but show similar tendencies as the climatology. The general large-scale patterns are consistent with the in-situ wind measurements (Figure 4c, f). However, a slight diversion towards northerly and south-westerly flow and lower wind speeds occurred in winter and summer (Figures 4c and f), respectively, when compared to the larger scale data (Figures 4b and d). In addition, south-westerly flows were more frequent in winter 2016 (Figures 4b and

c) than during the 30 year average climatology (Figure 4a), which had the potential to bring more polluted air in the upwind Hebei province to the observation sites in Beijing.

At 102 m, the flow is consistent with northerlies and north-westerlies in the winter campaign and dominantly southerly and easterlies during the summer campaign (Figure S1). The measured hourly mean wind speed, temperature and relative humidity were 3.1 m s^{-1}, 8.3 ^{o}C and 43.8 % in winter, and 3.6 m s, 25 ^{o}C and 46.7 % in summer, respectively. Typical diurnal patterns were observed with higher wind speed and temperature during the day and RH at night. During the winter haze events (defined in Figure 5) wind speed at 102 m were low (an average of 1.8 m s^{-1}) and mainly from the south-west direction (Figure S1).

5 . Air Quality During the Field Campaigns

5.1 Winter

During the winter campaign, the daily average concentration of $PM_{2.5}$ at IAP was 91.2 µg m^{-3} from the Partisol gravimetric measurements (Table 4) and 94.0 µg m^{-3} from an online FDMS (Filter dynamic measurement system). The maximum hourly $PM_{2.5}$ concentration was 438 µg m^{-3} (Figure 5 which shows the haze events listed in Table 5). $PM_{2.5}$ concentrations significantly exceeded both the daily air quality limit of China (75 µg m^{-3}) and WHO (25 µg m^{-3}). During the whole winter campaign period, nearly 50% of the hours had $PM_{2.5}$ mass concentration higher than 75 µg m^{-3} (Figure 5). The online PM_{10} concentration observed at the Olympic Park national air quality monitoring station was up to 560 µg m^{-3} during the campaign with an average of 130.6 µg m^{-3}. Average concentrations of NO_2, O_3, SO_2 and CO were 69.7 ± 33.3, 16.4 ± 17.0 and 14.9 ± 11.1 µg m^{-3} and 1.53 ± 1.02 mg m^{-3}, respectively (Table 4). Most of the criteria pollutants showed a similar temporal pattern (Figure 5), except O_3.

The daily average concentration of $PM_{2.5}$ was 99.7 µg m^{-3} at Pinggu (Table 4; based on Partisol gravimetric measurements). The maximum hourly $PM_{2.5}$ concentration was 617 µg m^{-3} (Figure 5). Similar to that at IAP, nearly 50% of the hours had $PM_{2.5}$ mass concentrations greater than 75 µg m^{-3}. Average concentrations of NO_2, O_3, SO_2 and CO are 46.4 ± 25.5, 22.3 ± 22.2, and 15.4 ± 6.7 µg m^{-3}, and 1.47 ± 1.17 mg m^{-3} respectively (Table 4). $PM_{2.5}$ was slightly higher at the rural site but NO, CO and SO_2 were comparable between the two sites. $PM_{2.5}$ and O_3 each had similar temporal patterns at the urban and rural sites (Figure 5), indicating a synoptic scale meteorological impact. The larger difference in the temporal variation of NO, NO_2 and SO_2 may reflect the varying contribution of more local sources. Large differences in temporal patterns of air pollutants were found on 4 December 2016 when $PM_{2.5}$, SO_2 and NO concentrations were much higher at Pinggu than at IAP.

Diurnal cycles of particles, NO_2 and CO showed no distinct peak but an increment during the nighttime, suggesting the possible impact of boundary layer and/or anthropogenic emissions in winter (Figure 6). The peak NO levels at 7 am are likely caused by the morning rush hour road traffic. $PM_{2.5}$ concentration increased sharply from 6 pm at Pinggu (not shown), suggesting important local emissions, likely domestic heating and cooking. SO_2 and O_3 had their highest levels in mid-morning or at noon (Figure 6).

Variations of particles, NO_x and SO_2 show that higher levels of these pollutants when air masses were from the south or southwest (Figure S2), indicating it was impacted by regional transport. All pollutants, except O_3, had higher mass concentrations when wind speeds were low, suggesting an influence from the local sources. The NO wind rose suggests a strong local source with little contribution from long-range transport. The O_3 concentration was higher during northerlies and when the concentrations of other pollutants such as NO_x and $PM_{2.5}$ were lower (Figure S2).

SNAQ box measurements at six levels (8 to 320 m) during the winter campaign (Figure 7) have similar overall temporal patterns of CO and NO to that measured by standard gas analyser (Figure 5). In most cases, the air pollutant levels are similar at different levels of the tower. There are notable differences in NO, CO and CO_2 on 11, 12 and 16 / 17 November, which suggests that the mixed layer height was low (e.g., <150 m). Interestingly, the O_x (NO_2 + O_3) levels are relatively homogeneous across the different levels. These measurements have implications on the role atmospheric chemistry play in transformation of species in the boundary layer, and the measurements also provide useful information that confirm mixed layer height determinations from independent methods such as the ceilometer (Table 1).

According to the meteorological standards (QX/T113-2010), haze is defined as: i) visibility < 10 km at relative humidity (RH) <80%; or ii) if RH is between 80 and 95%, visibility < 10 km and $PM_{2.5}$ > 75 μg m^{-3}. During the winter campaign 640 of the 1633 h were classified as haze periods using visibility data from Beijing Capital Airport (Figure S3); within the haze hours, 75% had $PM_{2.5}$ greater than 75 μg m^{-3} (Area A, Figure S3) and the rest had a visibility less than 10 km but with a RH <80% (Area B, Figure S3).

Characteristics of five major haze events during the winter campaign (Figure 5) show that $PM_{2.5}$, NO_2, SO_2 and CO had similar trends but O_3 levels dropped to very low concentration (<2 ppb). The events are defined in Table 5.

5.2 Summer

Concentrations of air pollutants excluding ozone during the summer campaign were much lower than in winter (Figure 8, Table 4). Average daily concentration of $PM_{2.5}$ and PM_{10} at IAP were 31.4 ± 14.7 and 74.9 ± 29.3 μg m^{-3} (based on gravimetric method), respectively. These levels were slightly higher than at Pinggu (27.8 ± 13.3 and 62.9 ± 29.3 μg m^{-3}). Concentrations of ozone were four to five times higher during the summer campaigns (106.9 ± 71.6 μg m^{-3} at IAP, and 91.8 ± 62.7 μg m^{-3} at Pinggu) than in the

winter campaign. Average concentration of NO_2, SO_2 and CO were 41.3 ± 23.5 and 6.3 ± 6.8 μg m^{-3} and 0.61 ± 0.32 mg m^{-3}at IAP respectively (Table 4). The concentrations of NO_2 and CO were lower at Pinggu while that of SO_2 was similar. All pollutants except $PM_{2.5}$ show more or less different temporal patterns (Figure 8), suggesting differences in sources at Pinggu and IAP during the summer campaign.

Diurnal patterns of NO, NO_2, and CO at IAP showed a distinct peak in the early morning, suggesting the contribution of traffic emissions (Figure 6). O_3 and O_x concentration peaked in mid-afternoon. The IAP $PM_{2.5}$ pollution rose suggests that both local and regional sources (from the south and south-east direction) impact the site (Figure S2). Unlike winter, high ozone concentrations occur during southerlies to southwesterlies, suggesting a regional source of this pollutant. NO and NO_x were largely from local sources during the summer campaign.

Characteristics of two minor haze events (IAP) during the summer campaign (Figure 8) are shown in Table 5.

5.3 Air quality in the Wider Beijing Megacity During the Field Campaigns

To assess if the IAP air quality is broadly representative of the wider Beijing megacity, variables were correlated with the 12 national air quality station data (Figure 9). A high correlation is observed with $PM_{2.5}$ across all sites except the rural background air quality station at Ming Tombs (G2, Figure 1); PM_{10}, CO and NO_2 at the urban sites are highly correlated but not with the rural and suburban sites (G2, G9 and G10, Figure 1) suggesting a more local source for these pollutants, comparing to $PM_{2.5}$ and O_3; SO_2 between sites shows a lower correlation compared to all other pollutants. The particularly high spatial correlations of both $PM_{2.5}$ and O_3 across almost all sites indicates a regional pollution phenomenon for the two pollutants. These results suggest that the air quality at the IAP urban site was broadly consistent with that at the other urban sites.

In general, $PM_{2.5}$ mass concentrations are similar at all the urban sites including IAP which are higher than at the suburban and rural background national monitoring sites (G2, G9 and G10, Figure S4). The Pinggu site has relatively high $PM_{2.5}$ pollution during the winter campaign but has the lowest concentrations during the summer campaign. This suggests that local anthropogenic sources have a major impact on $PM_{2.5}$ at this site during the winter campaign. Source apportionment results, notably high time resolution data are being used to explore this.

The $PM_{2.5}$ concentrations measured at IAP are highly correlated with those at the nearly national air quality station (Olympic Park, or Aotizhongxin, see Figure 1) (Figure S5), which gives confidence that

national air quality stations are of sufficient quality to provide valuable information on the spatial and temporal variation of key pollutants to supplement campaign measurements.

Table 4 shows that the IAP concentration data for all air quality variables are very close to the five year mean of the 12 national air quality monitoring stations. This lends further confidence that the chosen urban site represented well the overall pollution in the Beijing urban area.

5.4 Synoptic Circulation and Air Quality

The average mixed layer height observed at IAP varies with season and CT type (Figure 10a). Lower mixed layer height is usually linked to air pollution events. The 11 CTs (Section 4.3) are clearly associated with distinct air quality conditions based on analysis of hourly air quality data for 2013-2017 at one of the national urban air quality stations (G11, Olympic Park, Figure 1). Relatively low wind speeds of CT 7 may contribute to the long haze event from 15/11/2016 to19/11/2016 (Fig. 5). Most haze events during the winter campaign are cleared out by fresh air masses being advected from the North in CTs 3 or 5 (Figure 3), which is also marked by the increase in wind speed observed (Figure S1). Relatively lower $PM_{2.5}$ concentrations occurred (Figure 10b) under NE flow conditions (CTs 1-5), and higher concentrations during southerly flow (CTs 6-8, 10). The highest $PM_{2.5}$ concentrations occur during the heating season when regional flow showed stagnation (CT 9, 11). All haze events during the winter campaign (Figures 3&5) are dominated by those CTs although CTs with NE flow conditions occurred for short periods within the haze events (e.g. 18/11/2016, 04/12/2-16). Ozone levels are highest during CTs 5-8 (Figure **Error! Reference source not found.**10c), which predominate during spring and summer (Figure 10d).

In the Oct 2016 – Sept 2017 period (Figure 10e), the relative frequency of CTs differs slightly from the long-term climatology (Figure 10d). During the winter campaign, clean air advection from the NE (CTs 1-3) was less frequent than in the 30-y climatology. Given synoptic circulation types associated with stagnation do have a similar occurrence during the winter campaign compared to the same time period within the previous five years (with CT 9 8% less frequent and CTs 10 and 11 2% and 10% more frequent; Figure 10f), $PM_{2.5}$ concentrations were similar to the 5 year mean (Figure 10g, winter campaign period compared to the same dates during 2013-2017). During the summer campaign, south-north contrasts in geopotential were apparently reduced so CT 6 was 12% less frequent, while CT 7 was 11% more frequent (Figure 10f). The reduced advection of particles from southerly directions might have contributed to a 33% lower $PM_{2.5}$ concentrations compared to the five year average for the same time of year (Figure 10g). The relative decrease in O_3 (Figure 10g) during the winter campaign (24%) might be explained by cloud cover differences, which is being investigated.

5.5 Summary of Air Quality during the Campaigns

In summary, the winter campaign was characterised by several high $PM_{2.5}$ pollution events with peak hourly concentrations at the urban site ranging up to 617 µg m^{-3} (at Pinggu) whereas the summer experienced events of high ozone concentrations with the highest hourly average of 335 µg m^{-3} (at IAP) Air quality was generally poor during the winter campaign with an average $PM_{2.5}$ concentration of 91 µg m^{-3} in urban Beijing, but less severe than in the same period in 2015. Synoptic scale meteorological analysis suggests that the greater stagnation and weak southerly circulation in November/December 2016 contributed to the poor air quality during all haze events detected, and overall the $PM_{2.5}$ pollution level was similar to the five year average (2013-2017). $PM_{2.5}$ levels were relatively low during the summer campaign with the highest daily concentration of only 79 µg m^{-3}, matching the cleanest periods over the previous five years.

6. Preliminary Air Quality Modelling and Pollution Climatology of the Campaign Periods

Air quality modelling is a key component of the APHH-Beijing programme. A range of models have been applied that span global (UKCA, GEOS-Chem), regional (WRF-Chem, CMAQ, NAQPMS) and urban to street scales (ADMS). This section provides an example of the comparison between model simulated pollutant concentrations and APHH-Beijing observations made at IAP to demonstrate model capabilities. Results from specific modelling studies will be published separately.

Figure 11 shows that the magnitude and variation of wintertime $PM_{2.5}$ concentrations are reasonably reproduced by NAQPMS during the winter campaign, although there are some weakness in capturing the highest $PM_{2.5}$ levels during the haze events at the end of November and start of December. This is partly due to the representation of local meteorological features during this period, which bring these episodes to an end 6-12 hours early. The diurnal variations in O_3 during the summertime are reproduced relatively well by UKCA, which captures the rapid daytime formation of O_3 and strong nighttime removal. The very highest levels of daytime O_3 are underestimated with the model, particularly during the episode at the end of May. However, there is a strong local contribution to this as evident from the lower concentrations measured at Pinggu (Figure 8), and these local differences are not fully resolved with the model. Despite this, the day-on-day build-up of daytime O_3 during the periods of 22-27 May and 11-16 June is captured, and demonstrates that the model reproduces the synoptic drivers of local O_3 formation well.

We also investigated how representative the campaign periods were of the selected seasons in Beijing by comparing pollutant levels with those from the same period each year over the 2013-2017 period. The

NAQPMS model was run for the full 5-year period driven by NCEP meteorology and using temporally varying emissions for a single year that is broadly representative of 2013 conditions. The same emissions were used each year so that the meteorological contribution to pollutant levels could be assessed. This provides important information that cannot be obtained from the monitoring data (as emission varies year by year). The frequency distribution of $PM_{2.5}$ over each campaign period for each year is shown in Figure 12. Winter 2016 was broadly typical of the 5-year period, with similar characteristics to winter 2014, but both years show higher $PM_{2.5}$ under the same emissions than in 2013 or 2017. In addition, winter 2015 had substantially less favourable conditions for air quality, and more stagnant conditions led to three extended pollution episodes over the period with $PM_{2.5}$ exceeding 200 μg m^{-3}. In contrast, the summer period in 2017 was cleaner than average, with $PM_{2.5}$ levels very similar to 2015, and about 25% less than in 2013, 2014 or 2016. These results are broadly consistent with those based on synoptic weather analyses (section 5.4) as well as by Vu et al. (2019).

7. Summary

APHH-Beijing is an integrated and multidisciplinary research programme conducted by leading UK and Chinese researchers to (1) quantify sources and emissions of urban atmospheric pollutants; (2) elucidate processes affecting urban atmospheric pollution events; (3) estimate the personal exposure and impacts of air pollution on human health, and (4) develop intervention strategies to improve air quality and reduce health impacts in the Beijing megacity. This introduction paper outlines the motivation of the APHH-Beijing programme as well as providing the background air quality and meteorological conditions during the two intensive field campaigns that form the basis of data interpretation for campaign observations.

APHH-Beijing has measured the fluxes of key air pollutants, including NO_x, CO, BC, VOCs and speciated particulate matter, applied a suite of traditional and modern techniques to apportion the sources of particulate matter, determined a wide range of pulmonary and cardiovascular biomarkers linking to direct personal exposure and extensive fixed-station monitoring as well as source apportionment results, and has evaluated the effectiveness of Beijing's air pollution control policies using both chemical transport models and novel machine learning techniques. A number of papers have already been published by the APHH-Beijing programme including those in this special issue (Wang et al., 2019; Pan et al., 2019; Xia et al., 2018; Zhou et al., 2018; Wang et al., 2018b; Lyu et al., 2019; Hollaway et al., 2019; Du et al., 2018; Liu et al., 2018a,b; Smith et al., 2019; Vu et al., 2019; El zein et al., 2019). More papers are being prepared for publication in this special issue and elsewhere, which will cover (but are not limited to) emission fluxes of air pollutants, chemical composition and source apportionment of fine particles, satellite observations of trace gases and aerosols, sources and processes leading to haze events and photochemical smogs, physical and optical properties of aerosol particles, formation processes of secondary aerosols, urban meteorology, feedbacks between haze, photochemistry and meteorology,

integrated regional and urban scale modelling, personal exposure to air pollutants and human health effects of air pollution.

DATA DEPOSITORY

http://catalogue.ceda.ac.uk/uuid/7ed9d8a288814b8b85433b0d3fec0300

ACKNOWLEDGEMENT

Funding is provided by UK Natural Environment Research Council, Medical Research Council and Natural Science Foundation of China under the framework of Newton Innovation Fund (NE/N007190/1 (R Harrison, Z Shi, W Bloss); NE/N007077/1 (W Bloss)); NE/N00700X/1 (S Grimmond), NE/N007018/1 (F Kelly); NSFC Grant 81571130100(T Zhu), NE/N007115/1 (A C Lewis, A R Rickard, D C Carslaw); NE/N006917/1 (J D Lee, J F Hamilton, R E Dunmore); NE/N007123/1 (J Allan, C Percival, G McFiggans, H Coe); NE/N00695X/1 (C Percival, H Coe, G McFiggans, J Allan); NE/N006976/1 (N Hewitt, O Wild); NE/N006925/1 (O Wild); NE/N006895/1 (D Heard, L Whalley); NE/N00714X/1 (D Guan), NE/N007182/1 (M Loh); NSFC 41571130024 (P Fu) and NE/N006879/1 (P Palmer). Other Grant supports from Newton Fund/Met Office CSSP-China (S Grimmond; R Doherty and Z Shi), Royal Society Challenge Grant (CHG/R1/17003, Palmer) and NERC (NE/R005281/1, Shi) are acknowledged. Field help from Hong Ren, Qiaorong Xie, Wanyu Zhao, Linjie Li, Ping Li, and Shengjie Hou from IAP, Kjell zum Berge, Ting Sun at Reading University, Wu Chen, Yanwen Wang, Yunfei Fan, Teng Wang, Xi Che, Tao Xue, Pengfei Liang, Yingruo Li, Xinyan Hu, and Xinghua Qiu from Peking University, Li Yan, Hanbin Zhang, Yutong Cai, and Bingling Zhou from King's College London, Anika Krause from Cambridge University are also acknowledged. Many other staff and students from different institutions also contributed to the field campaigns and programme.

AUTHOR CONTRIBUTIONS

ZS drafted the manuscript and is the science coordinator of the APHH-Beijing programme. RMH, KBH, ACL, PQF, TZ, FJK, ML, ZWS, DBG and ST are lead PIs of the five research projects who led the funding applications and the research. They also drafted Section 2. TV plotted many of graphs and carried out the data analysis. SK, SG and MD carried out analysis and wrote Section 4.3 and 5.4; and YLW, MH, ZFW and OW carried out modelling and plotted Figure 11 and 12. PFQ, JL and ZT led the air quality measurements at the two measurements sites. SY, JL, RED, LR, DL, JA, DB, WJ, LC, LC, HC, TD, FKD, BZG, JFH, MH, DH, CNH, MH, DSJ, XJJ, RJ, MK, LK, BL, LC, JL, WJL, KDL, GM, MM, GM (Mills), JA, XFW, EN, BO, CP, PIP, OP, CR, CY, FL, JG, JC, LYS, YS, SRT, QQW, WHQ, XMW, ZFW, LW, XFW, ZJW, PHX, FMY, QZ, YLZ and MZ contribute to the field observations, laboratory measurements and / or modelling. ZS, SG, RMH., ZT, JL, OW, JA, JB, WJB, DC, DCC, HC, TD, RD, FKD, PQF, MFG, DBG, JFH, KBH, MH, DH, CNH, MH, XJJ, RJ, MK, FJK, LK, ACL, JL, ML, KL, GM (Mann), GM

(McFiggans), MM, PM, EN, FO, PIP, CP, CR, ARR, LYS, GYS, DS (Spracklen), DS (Stevenson), YS, XJW, JFL, BB, QC, ZWS, ST, SRT, XMW, ZFW, LW, ZJW, PHX, QZ, YHZ and MZ contributed to the funding applications, programme meetings and relevant programme research and/or supervision.

REFERENCES

Beck, C. and Philipp, A.: Evaluation and comparison of circulation type classifications for the European domain, Phys. Chem. Earth, Parts A/B/C, 35, 374-387, 2010.

Beekmann, M., Prévôt, A. S. H., Drewnick, F., Sciare, J., Pandis, S. N., Denier van der Gon, H. A. C., Crippa, M., Freutel, F., Poulain, L., Ghersi, V., Rodriguez, E., Beirle, S., Zotter, P., von der Weiden-Reinmüller, M. Bressi, S.-L.,, Fountoukis, C., Petetin, H., Szidat, S., Schneider, J., Rosso, A., El Haddad, I., Megaritis, A., Zhang, Q. J., Michoud, V., Slowik, J. G., Moukhtar, S., Kolmonen, P., Stohl, A., Eckhardt, S., Borbon, A., Gros, V., Marchand, N., Jaffrezo, J. L., Schwarzenboeck, A., Colomb, A., Wiedensohler, A., Borrmann, S., Lawrence, M., Baklanov, A. and Baltensperger U.: In situ, satellite measurement and model evidence on the dominant regional contribution to fine particulate matter levels in the Paris megacity. Atmos Chem Phys, 15, 9577-9591, 2015.

Bohn, B., Heard, D. E., Mihalopoulos, N., Plass-Dülmer, C., Schmitt, R., and Whalley, L. K.: Characterisation and improvement of $j(O^1D)$ filter radiometers, Atmos. Meas. Tech., 9, 3455-3466, 2016.

Bohnenstengel, S. I., Belcher, S. E., Aiken, A., Allan, J. D., Allen, G., Bacak, A., Bannan, T. J., Barlow, J. F.,Beddows, D. C. S., Bloss, W. J., Booth, A. M., Chemel, C., Coceal, O., Di Marco, C. F., Dubey, M. K., Faloon, K. H., Fleming, Z. L., Furger, M., Gietl, J. K., Graves, R. R., Green, D. C., Grimmond, C. S. B., Halios, C. H.,Hamilton, J. F., Harrison, R. M., Heal, M. R., Heard, D. E., Helfter, C., Herndon, S. C., Holmes, R. E., Hopkins, J. R., Jones, A. M., Kelly, F. J., Kotthaus, S., Langford, B., Lee, J. D., Leigh, R. J., Lewis, A. C., Lidster, R. T.,Lopez-Hilfiker, F. D., McQuaid, J. B., Mohr, C., Monks, P. S., Nemitz, E., Ng, N. L., Percival, C. J., Prevot, A. S. H., Ricketts, H. M. A., Sokhi, R., Stone, D., Thornton, J. A., Tremper, A. H., Valach, A. C., Visser, S., Whalley, L. K., Williams, L. R., Xu, L., Young, D. E. and Zotter, P.: Meteorology, air quality, and health in London: The ClearfLo project, B. Am. Meteorol Soc., 96, 779-804, 2014.

Brook, R. D., Brook, J. R., Urch, B., Vincent, R., Rajagopalan, S. and Silverman F.: Inhalation of fine particulate air pollution and ozone causes acute arterial vasoconstriction in healthy adults. Circulation. 105:1534-1536, 2002.

Chen, Y., Wenger, J. C., Yang, F., Cao, J., Huang, R., Shi, G., Zhang, S., Tian, M., and Wang H.: Source characterization of urban particles from meat smoking activities in Chongqing, China using single particle aerosol mass spectrometry, Environ Pollt, 228, 92-101, 2017.

Coyle, M., Nemitz, E., Storeton-West, R., Fowler, D., and Cape, J. N.: Measurements of ozone deposition to a potato canopy, Agri. Forest Meteoro., 149, 655-666, doi:10.1016/j.agrformet.2008.10.020, 2009.

Crilley, L.R., Kramer, L., Pope, F.D., Whalley, L.K., Cryer, D.R., Heard, D.E., Lee, J.D., Reed, C., Bloss, W.J.: On the interpretation of in situ HONO observations via photochemical steady state. Fara. Discuss., 189, 191-212, 2016.

Cryer, D.R., Measurements of hydroxyl radical reactivity and formaldehyde in the atmosphere, PhD Thesis, University of Leeds, 2016.

Dee, D. P., Uppala, S. M., Simmons, A. J., Berrisford, P., Poli, P., Kobayashi, S., Andrae, U., Balmaseda, M. A., Balsamo, G., Bauer, P., Bechtold, P., Beljaars, A. C. M., van de Berg, L., Bidlot, J., Bormann, N., Delsol, C., Dragani, R., Fuentes, M., Geer, A. J., Haimberger, L., Healy, S. B., Hersbach, H., Hólm, E. V., Isaksen, L., Kållberg, P., Köhler, M., Matricardi, M., McNally, A. P., Monge-Sanz, B. M., Morcrette, J.-J., Park, B.-K., Peubey, C., de Rosnay, P., Tavolato, C., Thépaut, J.-N. and Vitart, F.:

The ERA-Interim reanalysis: configuration and performance of the data assimilation system, Q. J. R. Meteorol. Soc., 137, 553-597, 2011.

Demuzere, M., Kassomenos, P. and Philipp, A.: The COST733 circulation type classification software: an example for surface ozone concentrations in Central Europe, Theor. Appl. Climatol., 105, 143-166, 2011.

Deventer, M. J., El-Madany, T., Griessbaum, F., and Klemm, O.: One-year measurement of size-resolved particle fluxes in an urban area, Tellus B: Chemical and Physical Meteorology, 67, 1, 25531, 10.3402/tellusb.v67.25531, 2015.

Du, W., Zhao, J., Wang, Y., Zhang, Y., Wang, Q., Xu, W., Chen, C., Han, T., Zhang, F., Li, Z., Fu, P., Li, J., Wang, Z., and Sun, Y.: Simultaneous measurements of particle number size distributions at ground level and 260 m on a meteorological tower in urban Beijing, China, Atmos. Chem. Phys., 17, 6797-6811, 10.5194/acp-17-6797-2017, 2017.

Du, H., Li, J., Chen, X., Wang, Z., Sun, Y., Fu, P., Li, J., Gao, J., and Wei, Y.: Modeling of aerosol property evolution during winter haze episodes over a megacity cluster in northern China: Roles of regional transport and heterogeneous reactions, Atmos. Chem. Phys. Discuss., https://doi.org/10.5194/acp-2018-1189, 2018.

Duan, J., Qin, M., Ouyang, B., Fang, W., Li, X., Lu, K., Tang, K., Liang, S., Meng, F., Hu, Z., Xie, P., Liu, W., and Häsler, R.: Development of an incoherent broadband cavity-enhanced absorption spectrometer for in situ measurements of HONO and NO_2, Atmos. Meas. Tech., 11, 4531-4543, 2018.

Dunmore, R. E., Hopkins, J. R., Lidster, R. T., Lee, J. D., Evans, M. J., Rickard, A. R., Lewis, A. C., and Hamilton, J. F.: Diesel-related hydrocarbons can dominate gas phase reactive carbon in megacities, Atmos. Chem. Phys., 15, 9983-9996, https://doi.org/10.5194/acp-15-9983-2015, 2015.

El zein, A., Dunmore, R.E., Ward, M.W., Hamilton, J.F., Lewis, A.C., Variability of polycyclic aromatic hydrocarbons and their oxidative derivatives in wintertime Beijing, China, Atmos. Chem. Phys. Discuss. https://doi.org/10.5194/acp-2019-120, 2019.

Fu, T.M., Jacob, D.J., Palmer, P.I., Chance, K., Wang,Y.X., Barletta, B., Blake, D.R., Stanton,J.C., Pilling, M.J.: Space‐based formaldehyde measurements as constraints on volatile organic compound emissions in east and south Asia and implications for ozone. J.Geophys. Res. – Atmos., D06312, doi:10.1029/2006JD007853, 2007.

GBD MAPS Working Group: Burden of Disease Attributable to Coal-Burning and Other Major Sources of Air Pollution in China. Special Report 20, Boston, MA, Health Effects Institute, 2016.

Ge, B., Sun, Y., Liu, Y., Dong, H., Ji, D., Jiang, Q., Li, J., and Wang, Z.: Nitrogen dioxide measurement by cavity attenuated phase shift spectroscopy (CAPS) and implications in ozone production efficiency and nitrate formation in Beijing, China, J. Geophys. Res., 118, 9499–9509, 10.1002/jgrd.50757, 2013.

Gerbig, C., Schmitgen, S., Kley, D., Volz-thomas, and Dewey, K.: An improved fast-response vacuum-UV resonance fluorescence CO instrument, J. Geophys. Res. 104, 1699-1704, 1999.

Guan, D., Su, X., Zhang, Q., Peters, G. P., Liu, Z., Lei, Y. and He K.: The socioeconomic drivers of China's primary $PM_{2.5}$ emission, Environ. Res. Lett, 9, 024010, 2014.

Han, T., Liu, X., Zhang, Y., Qu, Y., Gu, J., Ma, Q., Lu, K., Tian, H., Chen, J., Zeng, L., Hu, M., and Zhu, T.: Characteristics of Aerosol Optical Properties and Their Chemical Apportionments during CAREBeijing 2006, Aerosol Air Qual. Res., 14, 1431–1442, 2014.

Han, T., Xu, W., Li, J., Freedman, A., Zhao, J., Wang, Q., Chen, C., Zhang, Y., Wang, Z., Fu, P., Liu, X., and Sun, Y.: Aerosol optical properties measurements by a CAPS single scattering albedo monitor: Comparisons between summer and winter in Beijing, China, J. Geophys. Res., 122, 2513-2526, 10.1002/2016JD025762, 2017.

Högström, U., and Smedman, A.-S.: Accuracy of Sonic Anemometers: Laminar Wind-Tunnel Calibrations Compared to Atmospheric In Situ Calibrations Against a Reference Instrument, Boundary-Layer Meteoro., 111, 33-54, doi:10.1023/b:boun.0000011000.05248.47, 2004.

Hollaway, M., Wild, O., Yang, T., Sun, Y., Xu, W., Xie, C., Whalley, L., Slater, E., Heard, D., and Liu, D.: Photochemical impacts of haze pollution in an urban environment, Atmos. Chem. Phys. Discuss., https://doi.org/10.5194/acp-2019-29, 2019.

Hopkins, J.R., C.E. Jones, and A.C. Lewis, A dual channel gas chromatograph for atmospheric analysis of volatile organic compounds including oxygenated and monoterpene compounds, J. Environ. Monitor., 13, 2268-2276, 2011.

Huang, Z., Zhang, Y., Yan, Q., Zhang Z., and Wang X.: Real-time monitoring of respiratory absorption factors of volatile organic compounds in ambient air by proton transfer reaction time-of-flight mass spectrometry, J. Hazard. Mater., 320, 547-555, 2016.

Huth, R., Beck, C., Philipp, A., Demuzere, M., Ustrnul, Z., Cahynová, M., Kyselý, J. and Tveito, O. E.: Classifications of atmospheric circulation patterns, Ann. N. Y. Acad. Sci., 1146, 105-152, 2008.

Johnson, T., Capel, J., and Ollison, W.: Measurement of microenvironmental ozone concentrations in Durham, North Carolina, using a 2B Technologies 205 Federal Equivalent Method monitor and an interference-free 2B Technologies 211 monitor, J. Air & Waste Manag. Asso., 64, 360-371, doi:10.1080/10962247.2013.839968, 2014.

Junninen, H., Ehn, M., Petaja, T., Luosujarvi,L., Kotiaho, T., Kostiainen, R., Rohner, U., Gonin, M., Fuhrer, K., Kulmala, M., and Worsnop,D. R.: A high-resolution mass spectrometer to measure atmospheric ion composition, Atmos. Measure.Tech., 3, 1039–1053, 2010.

Kotthaus, S. and Grimmond, C. S. B.: Atmospheric boundary layer characteristics from ceilometer measurements part 1: A new method to track mixed layer height and classify clouds, Q. J. R. Meteorol. Soc., doi:10.1002/qj.3299, 2018a.

Kotthaus, S. and Grimmond, C. S. B.: Atmospheric boundary layer characteristics from ceilometer measurements part 2: Application to London's urban boundary layer, Q. J. R. Meteorol. Soc., doi:10.1002/qj.3298, 2018b.

Le Breton, M., Bacak, A., Muller, J. B. A., Bannan, T. J., Kennedy, O., Ouyang, B., Xiao, P., Bauguitte, S. J.-B., Shallcross, D. E., Jones, R. L., Daniels, M. J. S., Ball, S. M., Percival, C. J.: The first airborne comparison of N2O5 measurements over the UK using a CIMS and BBCEAS during the RONOCO campaign, Anal. Methods, 6, 9731-9743, 2014.

Le Breton, M., Wang, Y., Hallquist, Å. M., Pathak, R. K., Zheng, J., Yang, Y., Shang, D., Glasius, M., Bannan, T. J., Liu, Q., Chan, C. K., Percival, C. J., Zhu, W., Lou, S., Topping, D., Wang, Y., Yu, J., Lu, K., Guo, S., Hu, M., and Hallquist, M.: Online gas- and particle-phase measurements

of organosulfates, organosulfonates and nitrooxy organosulfates in Beijing utilizing a FIGAERO ToF-CIMS, Atmos. Chem. Phys., 18, 10355-10371, 2018.

Li, H.; Zhang, Q.; Duan, F.; Zheng, B.; and He. K. The "Parade Blue": effects of short-term emission control on aerosol chemistry, Faraday Discuss., 189, 317-335, 2016.

Li, M., Liu, H., Geng, G., Hong, C., Liu, F., Song, Y., Tong, D., Zheng, B., Cui H., Man, H., Zhang, Q., and He, K.: Anthropogenic emission inventories in China: a review, Nat. Sci. Rev., 4, 834-866, 2017.

Li, Z., Hu, R., Xie, P., Chen, H., Wu, S., Wang, F., Wang, Y., Ling, L., Liu, J., and Liu W.: Development of a portable cavity ring down spectroscopy instrument for simultaneous, in situ measurement of NO_3 and N_2O_5, Optics Express, 26, A433-A449, 2018.

Liang, P., Zhu, T., Fang, Y., Li, Y., Han, Y., Wu, Y., Hu, M., and Wang, J.: The role of meteorological conditions and pollution control strategies in reducing air pollution in Beijing during APEC 2014 and Victory Parade 2015, Atmos. Chem. Phys., 17, 13921-13940, 2017.

Lim, S.S., Vos, T., Flaxman, A.D., Danaei, G., Shibuya, K., Adair-Rohani, H., et al. 2012. A comparative risk assessment of burden of disease and injury attributable to 67 risk factors and risk factor clusters in 21 regions, 1990-2010: A systematic analysis for the global burden of disease study 2010, Lancet 380, 2224-2260, 2012.

Lin, W., Huang, W., Zhu, T., Hu, M., Brunekreef, B., Zhang ,Y., Liu, X., Cheng, H., Gehring, U., Li, C., and Tang, X.: Acute respiratory inflammation in children and black carbon in ambient air before and during the 2008 Beijing Olympics, Environ. Health Perspect., 119, 1507-12, 2011.

Linn, W. S. and Gong, Jr., H.: Air pollution, weather stress, and blood pressure, Am. J. Public Health, 91, 1345-1346, 2001.

Liu, D., Whitehead, J., Alfarra, M. R., Reyes-Villegas, E., Spracklen, D. V., Reddington, C. L., Kong, S., Williams, P. I., Ting, Y.-C., Haslett, S., Taylor, J. W., Flynn, M. J., Morgan, W. T., McFiggans, G., Coe, H. and Allan, J. D.: Black-carbon absorption enhancement in the atmosphere determined by particle mixing state, Nat. Geosci., 10, www.nature.com/naturegeoscience, 2017.

Liu, Y., Zheng, M., Yu, M., Cai, X., Du, H., Li, J., Zhou, T., Yan, C., Wang, X., Shi, Z., Harrison, R. M., Zhang, Q., and He, K.: High time resolution source apportionment of $PM_{2.5}$ in Beijing with multiple models, Atmos. Chem. Phys. Discuss., https://doi.org/10.5194/acp-2018-1234, 2018a.

Liu, D., Joshi, R., Wang, J., Yu, C., Allan, J. D., Coe, H., Flynn, M. J., Xie, C., Lee, J., Squires, F., Kotthaus, S., Grimmond, S., Ge, X., Sun, Y., and Fu, P.: Contrasting physical properties of black carbon in urban Beijing between winter and summer, Atmos. Chem. Phys. Discuss., https://doi.org/10.5194/acp-2018-1142, 2018b.

Lozano, R., Naghavi, M., Foreman, K., Lim, S., Shibuya, K., Aboyans, V., Abraham, J., Adair, T., Aggarwal, R., Ahn, S. Y., AlMazroa, M. A., Alvarado, M., Anderson, H. R., Anderson, L. M., Andrews, K. G., Atkinson, C., Baddour, L. M., Barker-Collo, S., Bartels, D. H., Bell, M. L., Benjamin, E. J., Bennett, D., Bhalla, K., Bikbov, B., Abdulhak, A. B., Birbeck, G., Blyth, F., Bolliger, I., Boufous, S., Bucello, C., Burch, M., Burney, P., Carapetis, J., Chen, H., Chou, D., Chugh, S. S., Coffeng, L. E., Colan, S. D., Colquhoun, S., Colson, K. E., Condon, J., Connor, M. D., Cooper, L. T., Corriere, M., Cortinovis, M., de Vaccaro, K. C., Couser, W., Cowie, B. C., Criqui, M. H., Cross, M., Dabhadkar, K. C., Dahodwala, N., De Leo, D., Degenhardt, L., Delossantos, A., Denenberg, J., Des Jarlais, D. C.,

Dharmaratne, S. D., Dorsey, E. R., Driscoll, T., Duber, H., Ebel, B., Erwin, P. J., Espindola, P., Ezzati, M., Feigin, V., Flaxman, A. D., Forouzanfar, M. H., Fowkes, F. G. R., Franklin, R., Fransen, M., Freeman, M. K., Gabriel, S. E., Gakidou, E., Gaspari, F., Gillum, R. F., Gonzalez-Medina, D., Halasa, Y. A., Haring, D., Harrison, J. E., Havmoeller, R., Hay, R. J., Hoen, B., Hotez, P. J., Hoy, D., Jacobsen, K. H., James, S. L., Jasrasaria, Jayaraman, R., S., Johns, N., Karthikeyan, G., Kassebaum, N., Keren, A., Khoo, J.-P., Knowlton, L. M., Kobusingye, O., Koranteng, A., Krishnamurthi, R., Lipnick, M., Lipshultz, S. E., Ohno, S. L., Mabweijano, J., MacIntyre, M. F., Mallinger, L., March, L., Marks, G. B., Marks, R., Matsumori, A., Matzopoulos, R., Mayosi, B. M., McAnulty, J. H., McDermott, M. M., McGrath, J., Memish, Z. A., Mensah, G. A., Merriman, T. R., Michaud, C., Miller, M., Miller, T. R., Mock, C., Mocumbi, A. O., Mokdad, A. A., Moran, A., Mulholland, K., Nair, M. N., Naldi, L., Narayan, K. M. V., Nasseri, K., Norman, P., O'Donnell, M., Omer, S. B.,. Ortblad, K, Osborne, R., Ozgediz, D., Pahari, B., Pandian, J. D., Rivero, A. P., Padilla, R. P., Perez-Ruiz, F., Perico, N., Phillips, D., Pierce, K., Pope III, C. A., Porrini, E., Pourmalek, F., Raju, M., Ranganathan, D., Rehm, J. T., Rein, D. B., Remuzzi, G., Rivara, F. P., Roberts, T., Rodriguez De León, F., Rosenfeld, L. C., Rushton, L., Sacco, R. L., Salomon, J. A., Sampson, U., Sanman, E., Schwebel, D. C., Segui-Gomez, M., Shepard, D. S., Singh, D., Singleton, J., Sliwa, K., Smith, E., Steer, A., Taylor, J. A., Thomas, B., Tleyjeh, I. M., Towbin, J. A., Truelsen, T., Undurraga, E. A., Venketasubramanian, N., Vijayakumar, L., Vos, T., Wagner, G. R., Wang, M., Wang, W., Watt, K., Weinstock, M. A., Weintraub, R., Wilkinson, J. D., Woolf, A. D., Wulf, S., Yeh, P.-H., Yip, P., Zabetian, A., Zheng, Z.-J., Lopez, A. D. and Murray C. J. L.: Global and regional mortality from 235 causes of death for 20 age groups in 1990 and 2010: a systematic analysis for the Global Burden of Disease Study 2010, The Lancet, 380(9859): 2095-128, 2013.

Lu, K. D., Rohrer, F., Holland, F., Fuchs, H., Bohn, B., Brauers, T., Chang, C. C., Häseler, R., Hu, M., Kita, K., Kondo, Y., Li, X., Lou, S. R., Nehr, S., Shao, M., Zeng, L. M., Wahner, A., Zhang, Y. H., and Hofzumahaus, A.: Observation and modelling of OH and HO2 concentrations in the Pearl River Delta 2006: a missing OH source in a VOC rich atmosphere, Atmos. Chem. Phys., 12, 1541-1569, doi:10.5194/acp-12-1541-2012, 2012.

Lu, K., Guo, S., Tan, Z., Wang, H., Shang, D., Liu, Y., Li, Xin, Wu, Z., Hu, M., Zhang, Y.: Exploring the atmospheric free radical chemistry in China: the self-cleansing capacity and the formation of secondary air pollution, Nat. Sci. Rev., 0: 1–16, doi: 10.1093/nsr/nwy073, 2018.

Lyu, R., Shi, Z., Alam, M. S., Wu, X., Liu, D., Vu, T. V., Stark, C., Fu, P., Feng, Y., and Harrison, R. M.: Insight into the Composition of organic compounds ($\geq C_6$) in $PM_{2.5}$ in wintertime in Beijing, China, Atmos. Chem. Phys. Discuss., https://doi.org/10.5194/acp-2018-1273, 2019.

McDermitt, D., Burba, G., Xu, L., Anderson, T., Komissarov, A., Riensche, B., Schedlbauer, J., Starr, G., Zona, D., Oechel, W., Oberbauer, S., and Hastings, S.: A new low-power, open-path instrument for measuring methane flux by eddy covariance, Appl. Phys. B, 102, 391-405, 10.1007/s00340-010-4307-0, 2011.

McManus, J. B., Zahniser, M. S., Nelson, D. D., Shorter, J. H., Herndon, S. C., Wood, E. C., and Wehr, R.: Application of quantum cascade lasers to high-precision atmospheric trace gas measurements, Opt. Eng., 49, 111124, doi: 10.1117/1.3498782, 2010

Meng, Z., Xu, X., Lin, W., Ge, B., Xie, Y., Song, B., Jia, S., Zhang, R., Peng, W., Wang, Y., Cheng, H., Yang, W., and Zhao, H.: Role of ambient ammonia in particulate ammonium formation at a rural site in the North China Plain, Atmos. Chem. Phys., 18, 167-184, 2018.

Miao, Y., Guo, J., Liu, S., Liu, H., Li, Z., Zhang, W. and Zhai, P.: Classification of summertime synoptic patterns in Beijing and their associations with boundary layer structure affecting aerosol pollution, Atmos. Chem. Phys, 17, 3097-3110, 2017.

Mills, G. P., Hiatt-Gipson, G. D., Bew, S. P., and Reeves, C. E.: Measurement of isoprene nitrates by GCMS, Atmos. Meas. Tech., 9, 4533–4545, 2016.

Moore, E., Chatzidiakou, L., Jones, R. L., Smeeth, L., Beevers, S., Kelly, F. J., Quint, J. K., Barratt, B.: Linking e-health records, patientreported symptoms and environmental exposure data to characterise and model COPD exacerbations: protocol for the COPE study, BMJ Open, 6, e011330,10.1136/bmjopen-2016-011330, 2016.

Nemitz, E., Hargreaves, K. J., McDonald, A.G., Dorsey, J. R., and Fowler, D.: Micrometeorological measurements of the urban heat budget and CO_2 emissions on a city scale, Environ. Sci. Technol., 36, 3139-3146, 2002.

Nemitz, E., Jimenez, J. L., Huffman, J. A., Ulbrich, I. M., Canagaratna, M. R., Worsnop, D. R. and Guenther, A. B.: An eddy-covariance system for the measurement of surface/atmosphere exchange fluxes of submicron aerosol chemical species - first application above an urban area, Aerosol Sci. Technol., 42, 636-657, 2008.

OECD, 2016. The economic consequences of outdoor air pollution - policy highlights. OECD Publishing, Paris, https://doi.org/10.1787/9789264257474-en.

Pan, X., Ge, B., Wang, Z., Tian, Y., Liu, H., Wei, L., Yue, S., Uno, I., Kobayashi, H., Nishizawa, T., Shimizu, A., Fu, P., and Wang, Z.: Synergistic effect of water-soluble species and relative humidity on morphological changes in aerosol particles in the Beijing megacity during severe pollution episodes, Atmos. Chem. Phys., 19, 219-232, https://doi.org/10.5194/acp-19-219-2019, 2019.

Pang, X., Lewis, A. C., Rickard, A. R., Baeza-Romero, M. T., Adams, T. J., Ball, S. M., Daniels, M. J. S., Goodall, I. C. A., Monks, P. S., Peppe, S., Ródenas García, M., Sánchez, P., and Muñoz A.: A smog chamber comparison of a microfluidic derivatisation measurement of gas-phase glyoxal and methylglyoxal with other analytical techniques, Atmos. Meas. Tech., 7, 373-389, 2014.

Palmer, P.I., Jacob, D.J., Fiore, A.M., Martin, R.V., Chance, K., Kurosu,T.P., Mapping isoprene emissions over North America using formaldehyde column observations from space. J. Geophys. Res.-Atmos., 108, D6, doi: 10.1029/2002JD002153, 2003.

Petäjä, T., Mordas, G., Manninen, H., Aalto, P. P., Hämeri, K., and Kulmala, M.: Detection Efficiency of a Water-Based TSI Condensation Particle Counter 3785, Aerosol Science and Technology, 40, 1090-1097, doi:10.1080/02786820600979139, 2006.

Philipp, A., Bartholy, J., Erpicum, M., Esteban, P., Fettweis, X., James, P., Jourdain, S., Kreienkamp, F., Krennert, T., Lykoudis, S., Michalides, S. C., Pianko-Kluczynska, K., Post, P., Álvarez, D. R., Schiemann, R., Spekat, A. and Tymvios, F. S.: Cost733cat – A database of weather and circulation type classifications, Phys. Chem. Earth, Parts A/B/C, 35(9–12), 360-373, 2010.

Philipp, A., Beck, C., Huth, R. and Jacobeit, J.: Development and comparison of circulation type classifications using the COST 733 dataset and software, Int. J. Climatol., 36(7), 2673-2691, 2016.

Popoola, O. A., Carruthers, D., Lad, C., Bright, V. B., Mead, I.M., Stettler, M., Saffell, J. and Jones, R.L.: The use of networks of low cost air quality sensors to quantify air quality in urban settings, Atmos. Environ., in review, 2018.

Shi, J.P., Harrison, R.M., Brear, F.: Particle size distribution from a modern heavy duty diesel engine, Sci. Total Environ., 235, 305-317, 1999.

Sloan, C. D., Philipp, T. J., Bradshaw, R. K., Chronister, S., Bradford Barber, W., and Johnston, J. D.: Applications of GPS-tracked personal and fixed-location PM2.5 continuous exposure monitoring, JAWMA, 66, 53-65, 2016.

Smith, K. R., Edwards, P. M., Evans, M. J., Lee, J. D., Shaw, M. D., Squires, F., Wilde, S., and Lewis, A. C.: Clustering approaches to improve the performance of low cost air pollution sensors, Faraday Discuss., 200, 621, 2017.

Smith, K. R., Edwards, P. M., Ivatt, P. D., Lee, J. D., Squires, F., Dai, C., Peltier, R. E., Evans, M. J., and Lewis, A. C.: An improved low power measurement of ambient NO_2 and O_3 combining electrochemical sensor clusters and machine learning, Atmos. Meas. Tech., 12, 1325-1336, , 2019.

Stone, D., Whalley, L. K., Ingham, T., Edwards, P. M., Crye,r D. R., Brumby, C. A., Seakins, P. W., Heard, D. E.: Measurement of OH reactivity by laser flash photolysis coupled with laser-induced fluorescence spectroscopy, Atmos. Measure. Tech., 9, 2827-2844, 2016.

Storer, M., Salmond, J., Dirks, K. N., Kingham, S., and Epton M.: Mobile selected ion flow tube mass spectrometry (SIFT-MS) devices and their use for pollution exposure monitoring in breath and ambient air–pilot study, J. Breath Res., 8, 037106 (7pp), doi:10.1088/1752-7155/8/3/037106, 2014.

Sun, Y. L., Wang, Z., Dong, H., Yang, T., Li, J., Pan, X., Chen, P., and Jayne, J. T.: Characterization of summer organic and inorganic aerosols in Beijing, China with an Aerosol Chemical Speciation Monitor, Atmos. Environ., 51, 250-259, 2012.

Sun, Y., Du, W., Fu, P., Wang, Q., Li, J., Ge, X., Zhang, Q., Zhu, C., Ren, L., Xu, W., Zhao, J., Han, T., Worsnop, D., and Wang, Z.: Primary and secondary aerosols in Beijing in winter: sources, variations and processes, Atmos. Chem. Phys., 16, 8309-8329, 2016.

Taiwo, A. M., Beddows, D. C. S., Calzolai, G., Harrison, R. M., Lucarelli, F., Nava, S., Shi, Z., Valli, G., and Vecchi, R.: Receptor modelling of airborne particulate matter in the vicinity of a major steelworks site, Sci. Tot. Environ., 490, 488-500, 2014.

Tan, Z., Fuchs, H., Lu, K., Hofzumahaus, A., Bohn, B., Broch, S., Dong, H., Gomm, S., Häseler, R., He, L., Holland, F., Li, X., Liu, Y., Lu, S., Rohrer, F., Shao, M., Wang, B., Wang, M., Wu, Y., Zeng, L., Zhang, Y., Wahner, A., and Zhang, Y.: Radical chemistry at a rural site (Wangdu) in the North China Plain: observation and model calculations of OH, HO2 and RO2 radicals, Atmos. Chem. Phys., 17, 663-690, 2017.

Tao, S., Ru, M. Y., Du, W., Zhu, X., Zhong, Q. R., Li, B. G., Shen, G. F., Pan, X. L., Meng, W. J., Chen, Y. L., Shen, H. Z., Lin, N., Su, S., Zhuo, S. J., Huang, T. B., Xu, Y., Yun, X., Liu, J. F., Wang, X. L., Liu, W. X., Chen, H. F., Zhu, D. Q.: Quantifying the Rural Residential Energy Transition in China from 1992 to 2012 through a Representative National Survey, Nat. Energy, 3, 567-573, 2018.

Tveito, O. E., and Huth, R.: Circulation-type classifications in Europe: results of the COST 733 Action, Int. J. Climatol., 36, 2671-2672, 2016.

Vanhanen, J., Mikkilä, J., Lehtipalo, K., Sipilä, M., Manninen, H. E., Siivola, E., Petäjä, T., and Kulmala, M.: Particle size magnifier for nano-CN detection, Aerosol Sci. Tech., 45, 533-542, 2011.

Vaughan, A. R., Lee, J. D., Misztal, P. K., Metzger, S., Shaw, M. D., Lewis, A. C., Purvis, R. M., Carslaw, D. C., Goldstein, A. H., Hewitt, C. N., Davison, B., Beeversh, S. D. and Karl, T. G.: Spatially resolved flux measurements of NO_x from London suggest significantly higher emissions than predicted by inventories, Faraday Discuss., 189, 455, 2016.

Vu, T.V., Shi, Z., Cheng, J., Zhang, Q., He, K., Wang, S., Harrison, R.M.; Assessing the impact of Clean Air Action Plan on Air Quality Trends in Beijing Megacity using a machine learning technique, Atmos. Chem. Phys. Discuss., https://doi.org/10.5194/acp-2019-173, 2019.

Wang, M., Zhu, T., Zheng, J., Y. Zhang, R., Zhang, S. Q., Xie, X. X., Han, Y. Q., and Li, Y.: Use of a mobile laboratory to evaluate changes in on-road air pollutants during the Beijing 2008 Summer Olympics, Atmos. Chem. Phys., 9, 8247-8263, 2009.

Wang, T., Nie, W., Gao, J., Xue, L.K., Gao, X.M., Wang, X.F., Qiu, J., Poon, C.N., Meinardi, S., Blake, D., Wang, S.L., Ding, A.J., Chai, F.H., Zhang, Q.Z., Wang, W.X.: Air quality during the 2008 Beijing Olympics: secondary pollutants and regional impact, Atmos. Chem. Phys., 10, 7603–7615, 2010.

Wang, M., Shao, M., Chen, W., Lu, S., Liu, Y., Yuan, B., Zhang, Q., Zhang, Q., Chang, C.-C., Wang, B., Zeng, L., Hu, M., Yang, Y., and Li, Y.: Trends of non-methane hydrocarbons (NMHC) emissions in Beijing during 2002-2013, Atmos. Chem. Phys., 15, 1489-1502, 2015a.

Wang, Q., Sun, Y., Jiang, Q., Du, W., Sun, C., Fu, P., and Wang, Z.: Chemical composition of aerosol particles and light extinction apportionment before and during the heating season in Beijing, China, J. Geophys. Res., 120, 12708-12722, 10.1002/2015JD023871, 2015b.

Wang, J., Zhang, Q., Chen, M.-D., Collier, S., Zhou, S., Ge, X., Xu, J., Shi, J., Xie, C., Hu, J., Ge, S., Sun, Y., and Coe, H.: First chemical characterization of refractory black carbon aerosols and associated coatings over the Tibetan Plateau (4730 m a.s.l), Environ. Sci. Technol., 51, 14072-14082, 2017a.

Wang, Y., Zhang, F., Li, Z., Tan, H., Xu, H., Ren, J., Zhao, J., Du, W., and Sun, Y.: Enhanced hydrophobicity and volatility of submicron aerosols under severe emission control conditions in Beijing, Atmos. Chem. Phys., 17, 5239-5251, 2017b.

Wang, W., Shao, L., Xing, J., Li, J., Chang, L. and Li, W.: Physicochemical characteristics of individual aerosol particles during the 2015 China victory day parade in Beijing, Atmosphere, 9, 40; doi:10.3390/atmos9020040, 2018a.

Wang, H., Lu, K., Chen, X., Zhu, Q., Wu, Z., Wu, Y., and Sun, K.: Fast particulate nitrate formation via N2O5 uptake aloft in winter in Beijing, Atmos. Chem. Phys., 18, 10483 10495, https://doi.org/10.5194/acp-18-10483-2018, 2018b.

Wang, J., Liu, D., Ge, X., Wu, Y., Shen, F., Chen, M., Zhao, J., Xie, C., Wang, Q., Xu, W., Zhang, J., Hu, J., Allan, J., Joshi, R., Fu, P., Coe, H., and Sun, Y.: Characterization of black carbon-containing fine particles in Beijing during wintertime, Atmos. Chem. Phys., 19, 447-458, https://doi.org/10.5194/acp-19-447-2019, 2019.

Whalley, L. K., Furneaux, K. L., Goddard, A., Lee, J. D., Mahajan, A., Oetjen, H., Read, K. A., Kaaden, N., Carpenter, L. J., Lewis, A. C., Plane, J. M. C., Saltzman, E. S., Wiedensohler, A., and

Heard D. E.: The chemistry of OH and HO_2 radicals in the boundary layer over the tropical Atlantic Ocean, Atmos. Chem. Phys., 10, 1555-1576, 2010.

WHO: Ambient air pollution: a global assessment of exposure and burden of disease. ISBN 978 92 151135 3, 2016a.

WHO: Burden of disease from joint household and ambient air pollution for 2012. http://www.who.int/phe/health_topics/outdoorair/databases/AP_jointeffect_methods_Nov2016.pdf?ua=1, 2016b.

Wragg, F. P. H., Fuller, S. J., Freshwater, R., Green, D. C., Kelly, F. J., and Kalberer M.: An automated online instrument to quantify aerosol-bound reactive oxygen species (ROS) for ambient measurement and health-relevant aerosol studies, Atmos. Meas. Tech., 9, 4891-4900, 2016.

Wu, Z. J., Poulain, L., Henning, S., Dieckmann, K., Birmili, W., Merkel, M., van Pinxteren, D., Spindler, G., Müller, K., Stratmann, F., Herrmann, H., and Wiedensohler, A.: Relating particle hygroscopicity and CCN activity to chemical composition during the HCCT-2010 field campaign, Atmos. Chem. Phys., 13, 7983-7996, 2013.

Wu, Z. J., Zheng, J., Shang, D. J., Du, Z. F., Wu, Y. S., Zeng, L. M., Wiedensohler, A., and Hu, M.: Particle hygroscopicity and its link to chemical composition in the urban atmosphere of Beijing, China, during summertime, Atmos. Chem. Phys., 16, 1123-1138, 2016.

Wu, J., Li, G., Cao, J., Bei, N., Wang, Y., Feng, T., Huang, R., Liu, S., Zhang, Q. and Tie, X.: Contributions of trans-boundary transport to summertime air quality in Beijing, China, Atmos. Chem. Phys., 17, 2035-2051, 2017.

Xia, Y., Guan, D., Jiang, X., Peng, L., Schroeder, H., Zhan, Q.: Assessment of socioeconomic costs to China's air pollution. Atmos. Environ. 139, 147-156, 2016.

Xia, Y., Guan, D., Meng, J., Li, Y., and Shan, Y.: Assessment of the pollution–health–economics nexus in China, Atmos. Chem. Phys., 18, 14433-14443, https://doi.org/10.5194/acp-18-14433-2018, 2018

Xie, C., Xu, W., Wang, J., Wang, Q., Liu, D., Tang, G., Chen, P., Du, W., Zhao, J., Zhang, Y., Zhou, W., Han, T., Bian, Q., Li, J., Fu, P., Wang, Z., Ge, X., Allan, J., Coe, H., and Sun, Y.: Vertical characterization of aerosol optical properties and brown carbon in winter in urban Beijing, China, Atmospheric Chemistry and Physics Discussions, 1-28, 10.5194/acp-2018-788, 2018.

Yang, G., Wang, Y., Zeng, Y., Gao, G. F., Liang, X., Zhou, M., Wan, X., Yu, S., Jiang, Y., Naghavi, M., Vos, T., Wang, H., Lopez, A. D., Murray, C. J. L.: Rapid health transition in China, 1990-2010: findings from the Global Burden of Disease Study 2010, The Lancet, 381, 1987-2015, 2013.

Yu, J., Yan, C., Liu, Y., Li, X., Zhou, T., Zheng, M.: Potassium: A Tracer for Biomass Burning in Beijing? Aerosol Air Qual. Res., 18, 2447-2459, 2018.

Yue, S., Ren, H., Fan, S., Sun, Y., Wang, Z. and Fu P.: Springtime precipitation effects on the abundance of fluorescent biological aerosol particles and HULIS in Beijing, Sci. Rep., 6, 29618, 10.1038/srep29618, 2016.

Zhang, Q., Streets, D. G., Carmichael, G. R., He, K. B., Huo, H., Kannari, A., Klimont, Z., Park, I. S., Reddy, S., Fu, J. S., Chen, D., Duan, L., Lei, Y., Wang, L. T., and Yao, Z. L.: Asian emissions in 2006 for the NASA INTEX-B mission, Atmos. Chem. Phys., 9, 5131-5153, 2009.

Zhang, J. B., Xu, Z., Yang, G., and Wang, B.: Peroxyacetyl nitrate (PAN) and peroxypropionyl nitrate (PPN) in urban and suburban atmospheres of Beijing, China, Atmos. Chem. Phys. Discuss., 11, 8173-8206, 2011.

Zhang, J. P., Zhu, T., Zhang, Q. H., Li, C. C., Shu, H. L., Ying, Y., Dai, Z. P., Wang, X., Liu, X. Y., Liang, A. M., Shen, H. X. and Yi, B. Q.: The impact of circulation patterns on regional transport pathways and air quality over Beijing and its surroundings, Atmos. Chem. Phys., 12, 5031-5053, 2012.

Zhang, Q., Jiang, X., Tong, D., Davis, S. J., Zhao, H., Geng, G., Feng, T., Zheng, B., Lu, Z., Streets, D. G., Ni, R., Brauer, M., van Donkelaar, A., Martin, R. V., Huo, H., Liu, Z., Pan, D., Kan, H., Yan, Y., Lin, J., He, K.and Guan, D.: Transboundary health impacts of transported global air pollution and international trade, Nature 543, 705-709, 2017a.

Zhang, Y., Ren, H., Sun, Y., Cao, F., Chang, Y., Liu, S., Lee, X., Agrios, K., Kawamura, K., Liu, D., Ren, L., Du, W., Wang, Z., Prevot, A. S. H., Szidat, S., and Fu, P.: High contribution of non-fossil sources to sub-micron organic aerosols in Beijing, China, Environ. Sci. Technol., 2017b.

Zhang, W.; Tong, S.; Ge, M.; An, J.; Shi, Z.; Hou, S.; Xia, K.; Qu, Y.; Zhang, H.; Chu, B.; Sun, Y.; He, H.: Variations and sources of nitrous acid (HONO) during a severe pollution episode in Beijing in winter 2016, Sci. Tot. Environ., 648, 253-262, 2019.

Zhao, W., Kawamura, K., Yue, S., Wei, L., Ren, H., Yan, Y., Kang, M., Li, L., Ren, L., Lai, S., Li, J., Sun, Y., Wang, Z., and Fu P.: Molecular distribution and compound-specific stable carbon isotopic composition of dicarboxylic acids, oxocarboxylic acids and α-dicarbonyls in $PM_{2.5}$ from Beijing, China, Atmos. Chem. Phys., 18, 2749–2767, 2018.

Zhou, W., Zhao, J., Ouyang, B., Mehra, A., Xu, W., Wang, Y., Bannan, T. J., Worrall, S. D., Priestley, M., Bacak, A., Chen, Q., Xie, C., Wang, Q., Wang, J., Du, W., Zhang, Y., Ge, X., Ye, P., Lee, J. D., Fu, P., Wang, Z., Worsnop, D., Jones, R., Percival, C. J., Coe, H., and Sun, Y.: Production of N_2O_5 and $ClNO_2$ in summer in urban Beijing, China, Atmos. Chem. Phys., 18, 2018.

TABLE LEGENDS:

Table 1: Overview of measurements in APHH-Beijing at the urban site.

Table 2 Overview of measurements at the Pinggu site.

Table 3: Mean and standard deviation (sd) of climatological conditions in Beijing for each circulation type (CT) for 1988-20 17 from ERA-Interim data with frequency of the CT during the W (winter) and S (summer) campaigns (% of 6 h periods (p)) compared to long- term (1988-2017) averages.

Table 4: Haze periods during the summer and winter campaign periods.

Table 5: Average air quality variables at IAP, Pinggu and 12 national monitoring sites (12N) during the field campaigns (10 November – 11 December 2016; and 21 May – 22 June 2017). The 12 national sites five-year mean concentrations for same times of the years (12N -5Y) and for the same time of the year (campaign period) (12N-campaign). Data are mean ± s.d. (range).

FIGURE LEGENDS

Figure 1: Study area topography (source: googlemap) of Beijing / Tianjing / Hebei region (a) with the rectangle showing enlarged study area; locations of measurement sites (Institute of Atmospheric Physics (IAP)– urban Beijing, Pinggu – rural Beijing; and Gucheng – upwind site in Hebei province), SNAQ box sites (red symbols) and the 12 national air quality monitoring stations (G1 to G12, blue symbols) (b).. The shaded area shows the Beijing builtup area. (Source: a and b - Goggle Map topographic background imagery; c – taken by Jian Zhao from IAP). G1: Wangshouxigong; G2: Dingling (Ming Tombs); G3: Dongsi; G4: Tiantan; G5: Nongzhanguan; G6: Guanyuan; G7: Haidianquwanliu; G8: Shunyxicheng; G9: Huairouzhen; G10:Changpingzhen; G11: Aotizhongxin (Olympic Park); G12: Gucheng. Categories: Urban: G1, G3, G4, G5, G6, G7, G8, G11, G12; Suburban: G9, G10; Rural: G2.

Figure 2: ERA-Interim (1988-2017) average 925 hPa geopotential with 10 m horizontal wind

vector for 11 circulation types classified for Beijing (municipal boundary thin solid line) surroundings (103-129° E, 31 - 49° N) determined with the SANDRA method (COST733 class software). Frequency of occurrence is given in cluster caption. For discussion of conditions associated with each CT see Section 4.3.

Figure 3: Time series of circulation types (CTs) during the two field campaigns: (a) winter and (b) summer. The 11 CTs are shown in Figure 2. See text for more description. Shading shows the pollution events identified in Section 5 and Figure 5.

Figure 4: Beijing wind roses: (a, b, d, e) ERA-Interim 10 m horizontal wind (40° N, 116.5° E) and (c, f) sonic anemometer (Table 1) at IAP 320 m agl for (a) 5 November – 10 December in 1988-2017, (d) 15 May – 22 June in 1988-2017, (b, c) 5 November – 10 December 2016, and (e, f) 15 May – 22 June 2017.

Figure 5: Time-series of air quality variables at the urban and rural sites during the winter campaign; Five haze events are indicated (shading; see also Table 4).

Figure 6: Diurnal patterns of gaseous pollutants normalized by average concentrations at IAP during winter and summer campaigns. Line shows the mean concentrations and shaded area as 95% confidence interval in the difference in mean concentrations

Figure 7: Time series of CO_2, CO, NO, O_x (NO_2+O_3) and wind speed at six heights (colour) measured with SNAQ boxes on the IAP tower during the winter intensive field campaign.

Figure 8: Time-series of air quality variables at the urban and rural sites during the summer campaign. Two minor haze events are indicated (shading).

Figure 9: Correlations between the air quality at IAP, PQ and 12 monitoring station around Beijing. Stations G1-G12 (Figure 1(b)) are labelled 01-12, PG = Pinggu.

Figure 10: Analysis by circulation type (CT; Sect. 4.3) of: (a) daily maximum mixed layer height (MLH) determined from ALC observations at IAP between November 2016 – June 2017 (analysis method, Kotthaus and Grimmond, 2018b); concentration of (b) $PM_{2.5}$ and (c) O_3 at the Olympic Park (i.e. Aotizhongxin) in 2013-2017 from the national air quality

network for different CTs; occurrence of CTs in (d) 1988-2017 and (e) Oct 2016 – Sept 2017; (f) anomaly of CT frequency during the campaigns compared to 5 y (2013-2017) averages; and (g) anomaly of $PM_{2.5}$ and O_3 during the campaigns compared to 5 y (2013-2017) averages. IOP = intensive observation period (i.e., campaign period).

Figure 11: Comparison of observed (at IAP) and modelled pollutant concentrations showing (a) $PM_{2.5}$ concentrations during the winter campaign compared with NAQPMS simulations, and (b) O_3 mixing ratios in summer compared with UKCA simulations.

Figure 12: Frequency distribution of $PM_{2.5}$ in Beijing over the winter (top) and summer (bottom) campaign periods from the NAQPMS model compared with those from the same periods over the past five years under the same emission conditions.

Table 1: Overview of measurements in APHH-Beijing at the urban site.

	Instrument	Measurements	Institute	References
Container 2	FAGE	OH (Chem and Wave)^{X}, HO_2, RO_2	Leeds	Whalley et al. (2010)
	OH reactivity	OH reactivity	Leeds	Stone et al. (2016)
	Spectral radiometer	Photolysis rates	Leeds	Bohn et al. (2016)
	Filter radiometer	$J(O^1D)$	Leeds	Bohn et al. (2016)
	Dew point hygrometer	Water vapour	Leeds	Whalley et al. (2010)
	Davis met station	Wind speed, direction, temp, RH, pressure	Leeds	
	Vaisala CL31 ALC Ceilometer $^{+}$	Cloud-base height, mixing height, attenuated backscatter profiles	Reading	Kotthaus and Grimmond (2018a)
	Personal air monitors (PAMS)	CO, NO, NO_2, PM_1, PM_{10}, $PM_{2.5}$	Cambridge	Moore et al. (2016)
	MicroPEMs	Personal PM exposure	IOM	Sloan et al. 2015
Container 2	DC-GC-FID	C2-C7 VOCs and oVOCs	York	Hopkins et al. (2011)
	GCxGC FID	C6 - C13 VOCs and oVOCs	York	Dunmore et al. (2015)
	TEI 42i	NO	Birmingham	
	Teledyne CAPS	NO_2	York	
	TEI 42c	Total NO_y	York	
	TEI 49i	O_3	York	
	TEI 43i	SO_2	York	
	Sensor box	CO	York	Smith et al. (2017)
	BBCEAS	HONO, NO_3, N_2O_5	Cambridge	Le Breton et al. (2014)
Container 3	LOPAP	HONO	Birmingham	Crilley et al. (2016)
	LIF HCHO	HCHO	Leeds	Cryer et al. 2016
	LOPAP	HONO	IC-CAS	Zhang et al. (2019)
	GC-MS	Organic nitrates	East Anglia	Mills et al. (2016)
	ROS online analyser	Reactive Oxygen Species	Cambridge	Wragg et al. (2016)
Container	FAGE	OH (wave)^{x}, HO_2	Peking	Lu et al., 2012

	FAGE	OH (chem)[x]	Peking	Tan et al., 2017
	TEI 42i	NO	Peking	Tan et al., 2017
	Teledyne CAPS	NO2	Peking	
	TEI 42c with Moly converter	NO_2	Peking	
	TEI 49i	O_3	Peking	
	TEI	CO	Peking	
	Spectral radiometer	Photolysis rates	Peking	
	GC-ECD	PAN	Peking	Zhang et al., 2011
	GC-MS	VOCs	Peking	Wang et al., 2015a
Container 5 *	H-TDMA/V-TDMA	Hygroscopicity/volatility	Peking	Wu et al., 2013
	SMPS+APS	Particle Number size distribution	Peking	Wu et al., 2016
	Particle size magnifier	Size distribution of < 3nm particles	Peking	Vanhanen et al., 2011
	IGAC-IC	Water-soluble ions	Peking	Yu et al. (2018)
	Xact	Metal	Peking	Yu et al. (2018)
	Sunset OC/EC	EC/OC	Peking	Zhang et al. (2017b)
Container 6	IBBCEAS	HONO, NO_2	AIOFM	Duan et al. (2018)
	CRDS	NO_3 and N_2O_5	AIOFM	Li et al. (2018)
	Nitrate Api-TOF-CIMS	Organics, clusters (HOMs)	Birmingham	Junninen et al. (2010)
	SMPS	Particle size distribution	Birmingham	Shi et al. (1999)
	Particle size magnifier	Size distribution of < 3 nm particles	Birmingham	Vanhanen et al. (2011)
Container 7	Fast NO_x	NO_x fluxes	York	Vaughan et al. (2016)
	AL5002 CO analyser	CO fluxes	York	Gerbig et al. (1999)
	HR-TOF-AMS	Fluxes of PM_1 non-refractory (NR) species	CEH	Nemitz et al. (2008)
	SP2	BC fluxes	Manchester	Liu et al. (2017)
	PTR-TOF-MS	VOC fluxes	GIG Lancaster	Huang et al. (2016)

	SYFT-MS Voice 200 Ultra	VOC fluxes	York	Storer et al. (2014)
Container 8	SMPS3968-APS3321	Particle number size distribution	BNU	Du et al. (2017)
	H/V TDMA	Particle hygroscopicity	BNU	Wang et al. (2017b)
	CCNC-100	CCN	BNU	Wang et al. (2017b)
	PAX (870nm)	Extinction & absorption coefficient	IAP	Xie et al. (2018)
	Ammonia analyzer	NH_3	IAP	Meng et al. (2018)
	Sunset OC/EC analyzer	Online OC/EC	IAP	Zhang et al. (2017b)
Container 9	Iodide FIGAERO-TOF-CIMS	Particle and gas phase molar molecule	Manchester	Le Breton et al. (2018)
	CPMA-SP2	Black carbon mass and mixing state	Manchester	Liu et al. (2017)
	Micro reactor	oVOCs	York	Pang et al. (2014)
Tower ~100 m	QCL NH_3	Ammonia fluxes	CEH	McManus et al. (2010)
	IRGA LiCOR-7500	CO_2 / H_2O flux	CEH	McDermitt et al. (2011)
	DMT UHSAS	Size resolved particle flux (0.06-1 µm)	CEH	Deventer et al. (2015)
	TSI APS3021	Size-resolved particle flux (0.5-25 µm)	CEH	Nemitz et al., (2002)
	TSI CPC3785	Total particle number flux	CEH	Petäjä et al., (2006)
	ROFI	O_3 flux	CEH	Coyle et al., 2009
	Sonic anemometer R3-50	Turbulence, sensible heat flux	CEH	Högström and Smedman (2004)
	WXT530 weather station	T, P, RH, wind speed & direction, precipitation	CEH	

	2B O_3 analyser	O_3 concentration	CEH	Johnson et al. (2014)
Tower ~120 m	High-vol sampler	$PM_{2.5}$ filter samples	IAP	
	Anderson sampler	Size-resolved PM samples	IAP	
Tower ~260 m	High-vol sampler	$PM_{2.5}$ filter samples	IAP	
	Anderson sampler	Size- resolved PM samples	IAP	
	ACSM	NR PM_1 species	IAP	Sun et al. (2012)
	CAPS-PM-$_{Ext}$ (630nm)	Extinction	IAP	Wang et al. (2015b)
	SMPS 3938	Particle Number size distribution	IAP	Du et al. (2017)
	Gas analyser	CO, O_3 and SO_2	IAP	Zhou et al. (2018)
	Aethalometer AE33	Black carbon	IAP	Xie et al. (2018)
	Single particle sampler	Individual particles	CUMTB	Wang et al. (2018a)
Tower and tower basket measurements	SNAQ boxes (x 6 at different heights)	CO, NO, NO_2, SO_2, PM_1, PM_{10}, $PM_{2.5}$	Cambridge	Popoola et al. (2018)
	LOPAP	HONO (3 min avg)	Birmingham	Crilley et al. (2016)
	Spectral radiometer	Photolysis rates	Leeds	Bohn et al. (2016)
	SNAQ	CO, NO, NO_2, SO_2, PM_1, PM_{10}, $PM_{2.5}$	Cambridge	Popoola et al. (2018)
	WIBS	Fluorescent biological aerosol particles (FBAP)	IAP	Yue et al. (2016)
	AE33	BC	IAP	Xie et al. (2018)
	Los Gatos NH_3 Analyzer	NH_3	IAP	Meng et al. (2018)
	PAX	Light scattering / absorption	IAP	Xie et al. (2018)
IAP ground	High-Vol sampler	$PM_{2.5}$ filter samples	Peking	
	4-channel sampler	$PM_{2.5}$ filter samples	Peking	

	High Vol sampler	*High time resolution $PM_{2.5}$* filter samples	York	
IAP roof/lab	FDMS+Thermo Scientific 1405-DF	Online $PM_{2.5}$ mass conc.	IAP	
	Partisol sampler	$PM_{2.5}$ + $PM_{2.5-10}$	Birmingham	Taiwo et al. (2014)
	Streaker sampler	Hourly elements in $PM_{2.5}$ and $PM_{2.5-10}$	Birmingham	Taiwo et al. (2014)
	Digitel High Vol	$PM_{2.5}$ daily	IAP	
	Digitel High Vol	PM_1 - 3 hourly	IAP	
	Andersen sampler	Size resolved PM	IAP	
	WIBS	Fluorescent biological particles	IAP	Yue et al. (2016)
	CAPS-NO_2	NO_2	IAP	Ge et al. (2013)
	Aethalometer AE33	Black carbon	IAP	Xie et al. (2018)
	CAPS-PM_{SSA} (630nm)	Extinction, Scattering	IAP	Han et al. (2017)
	HR-ToF-AMS	NR-PM species	IAP	Sun et al. (2016)
	SP-AMS	Refractory BC and coated aerosol composition		Wang et al. (2017a)
	Iodide FIGAERO-ToF-CIMS	Particle and gas phase molar molecule	IAP	Zhou et al. (2018)
	Single particle sampler	Individual particles	CUMTB	Wang et al. (2018)

Institution names: AIOFM = Anhui Institute of Fine Optics and Mechanics; BNU = Beijing Normal University; CEH = Centre for Ecology and Hydrology; CUMTB = China University of Mining and Technology (Beijing); GIG = Guangzhou Institute of Geochemistry, Chinese Academy of Sciences; NUIST = Nanjing University of Information Science &Technology; IC-CAS = Institute of Chemistry, Chinese Academy of Sciences

[+] Deployment of instruments both campaigns unless: 10/11/2016 to 25/6/2017

[*] Winter campaign only

[X] OH wave and OH chem refer to the method used to obtain the background signal for the FAGE instruments which are equipped with a scavenger inlet

Table 2: Overview of measurements at the Pinggu site.

Instruments	Measurements	Insitutue	Reference
Thermo gas analysers	$NO_x/SO_2/CO/O_3$	Peking	Liang et al., 2017
BAM 1020	$PM_{2.5}$ mass concentration	Peking	Liang et al., 2017
High vol sampler	$PM_{2.5}$ samples	IAP	Zhao et al., 2018
Medium vol sampler	$PM_{2.5}$ samples	IAP	Zhao et al., 2018
Low vol Andersen sampler	Size resolved PM samples	IAP	Zhao et al., 2018
Partisol sampler	$PM_{2.5}$ samples	Birmingham	Taiwo et al. (2014)
Streaker sampler	Hourly elements in $PM_{2.5}$ and $PM_{2.5\text{-}10}$	Birmingham	Taiwo et al. (2014)
High vol sampler	Filters of $PM_{2.5}$; high time resolution	Birmingham	
Four Channel sampler	$PM_{2.5}$ samples	Peking	Liang et al., 2017
Thermo MAAP	Online Black Carbon	Peking	Lin et al., 2011
Sunset OC/EC analyzer	Online OC/EC	Peking	Han et al., 2014
Xact	Hourly metals	Peking	Yu et al. (2018)
TOF-ACSM	NR-chemical composition (summer)	Peking	Sun et al., 2012
Thermo Metone	Meteorological parameters	Peking	Liang et al., 2017
SNAQ	Meteorological parameters	Cambridge	Popoola et al. (2018)
SP-AMS	Individual particle composition	CQIGIT	Chen et al. (2017)
SMPS	Size distribution	Tsinghua	Wang et al., 2009
ACSM	NR-chemical composition (winter)	Tsinghua	Li et al. (2016)

CQIGIT = Chongqing Institute of Green and Intelligence Technology, Chinese Academy of Sciences

Table 3: Mean and standard deviation (sd) of climatological conditions in Beijing for each circulation type (CT) for 1988-2017 from ERA-Interim data with frequency of the CT during the W (winter) and S (summer) campaigns (% of 6 h periods (p)) compared to long- term (1988-2017) average-A

		WS	WS_{sd}	WD	WD_{sd}	T2m	$T2m_{sd}$	TD2m	$TD2m_{sd}$	MSLP	$MSLP_{sd}$	RH	RH_{sd}	Season	Frequency (%)		
CT	Description	m s^{-1}	m s^{-1}	°	°	°C	°C	°C	°C	hPa	hPa	%	%		W	S	A
1	H - west of the domain	3.38	1.63	298.3	62.6	0.1	7.1	-12.6	7.9	1026.50	4.14	41	18	Winter monsoon	16	7	9.3
2	H - west of the domain	2.91	1.49	265.9	107.0	-2.8	6.2	-13.8	7.5	1034.34	4.47	45	18	Winter monsoon	1	0	7.2
3	relatively L in NE	3.21	1.65	281.2	71.3	6.8	8.9	-6.4	9.3	1017.77	4.35	43	20	Sep- May	12.5	0	8.3
4	further reduction L (cf. CT3, 5) in NE winds start to turn over Yellow Sea	3.05	1.73	240.1	104.1	19.2	7.5	7.0	10.4	1007.20	3.63	50	24	Mar-Aug Spring - summer	11.8	4	7.8
5	relatively L in NE	2.57	1.37	189.1	125.0	8.2	8.9	-0.9	10.4	1020.82	4.62	57	23	Sep-May	7.6	34	8.3
6	further reduction L (cf. CT3, 5) in NE	2.58	1.32	197.4	87.6	24.6	5.9	14.7	8.0	1000.99	2.96	59	23	Summer monsoon	8.3	12	8.9
7	when winds are oriented westward from the Bohai Sea	2.29	1.12	167.5	100.2	18.9	7.8	10.7	9.5	1012.59	3.61	63	21		1 p	11	10.2
8	like CT 6	2.35	1.11	165.4	75.4	24.0	5.3	15.9	6.8	1006.47	2.69	65	21	Summer monsoon		32	12.9
9	Air mass stagnant over Beijing	2.03	0.94	208.7	107.4	2.1	7.9	-6.2	8.4	1028.66	4.18	58	20			0	9.6
10	Air mass stagnant over Beijing	2.67	1.17	211.1	68.7	14.2	9.4	3.1	10.0	1013.98	3.84	52	22		25	0	7.2

11	Air mass stagnant over Beijing	2.23	0.98	209.1	86.5	8.1	9.4	-0.4	9.6	1021.83	4.06	59	20		16	0	10.3

Note: WS- wind speed, WD wind direction, T2m – 2 m air temperature, TD2m – 2 m dewpoint temperature, MSLP – mean sea level pressure, RH – relative humidity; L – low pressure; H – High pressure

Table 4: Average air quality variables at IAP, Pinggu and 12 national monitoring sites (12N) during the field campaigns (10 November – 11 December 2016; and 21 May – 22 June 2017). The 12 national sites five-year mean concentrations for same times of the years (12N -5Y) and for the same time of the year (campaign period) (12N-campaign). Data are mean ± s.d. (range).

Pollutant[1]	**Winter** *(10 Nov-11 Dec 2016)*				**Summer** *(21 May-22 June 2017)*			
	IAP	PG	12N-5Y	12N - campaign	IAP	PG	12N-5Y	12N- campaign
$PM_{2.5}$ [2]	91.2 ± 63.7 (10.3-239.9)	99.7 ± 77.8 (13.3-294.3)	84.01 ± 89.1 (3.2-593.3)	95.3 ± 79.6 (4.7-408.8)	31.4 ± 14.7 (12.2-78.8)	27.8 ± 13.3 (10.6-70.3)	58.7 ± 40.0 (4.2-250.3)	41.7 ± 22.3 (8.9- 134.1)
PM_{10} [2]	130.6 ± 87.0 (20.0-329.2)	121.9 ± 80.4 (10.4-312.1)	112.8 ± 102.2 (5-662.0)	134.5 ± 100.4 (6.0-550.1)	74.9 ± 29.3 (22.5-164.6)	62.9 ± 29.3 (15.1-141.9)	94.6 ± 52.7 (5.0-463.2)	81.9 ± 37.1 (6.0-277.8)
NO_2	69.7 ± 33.3 (10.2-167.3)	46.4 ± 25.5 (2.3-132.4)	57.7 ± 33.9 (3.9-166.4)	66.4 ± 31.3 (7.3-156.6)	41.3 ± 23.5 (9.2-142.9)	29.3 ± 10.3 (9.3-84.0)	40.6 ± 17.9 (8.1-132.4)	37.6 ± 16.2 (12.5-92.8)
SO_2	14.9 ± 11.1 (0.1-50.8)	15.4 ± 6.7 (6.2-44.4)	16.6 ± 16.2 (1.4-112.0)	14.2 ± 9.4 (2.1-51.4)	6.3 ± 6.8 (0.1-38.2)	8.9 ± 4.7 (4.2-41.2)	10.1 ± 10.6 (1.8-82.3)	7.4 ± 6.6 (1.8-64.5)
CO	1.53 ± 1.02 (0.7-5.0)	1.47 ± 1.17 (0.1-6.9)	1.65 ± 1.38 (0.1-9.6)	1.86 ± 1.17 (0.3-5.7)	0.61 ± 0.32 (0.1-2.5)	0.52 ± 0.29 (0.1-2.3)	0.93 ± 0.74 (0.2-8.7)	0.74 ± 0.33 (0.2-2.5)
O_3	16.4 ± 17.0 (0.3-63.3)	22.3 ± 22.2 (2.9-78.0)	21.8 ± 20.5 (1.0-72.9)	17.5 ± 19.2 (2.1-67.4)	106.9 ± 71.6 (2.0-349.3)	91.8 ± 62.7 (0.2-291.4)	100.4 ± 67.8 (2.2-343.5)	110.8 ± 66.5 (3.6-335.9)

[1], Units: μg m^{-3} except CO units: mg m^{-3}

[2], $PM_{2.5}$ and PM_{10} from IAP and Pinggu measured by a gravimetric method; all other data are online measurements hourly mean.

1298

Table 5: Haze periods during the summer and winter campaign periods.

Event	Time	$PM_{2.5}$ (μg m^{-3})	Visibility (km)
Winter Haze Event 1	11/08 21:00- 11/10 16:00	158 (79 - 229)	4.1 (2.3-8)
Winter Haze Event 2	11/15 21:00- 11/19 08:00	143 (56 - 244)	4.2(0.6-8)
Winter Haze Event 3	11/24 12:00- 11/27 02:00	210 (68-363)	4.2(1.5-8)
Winter Haze Event 4	12/02 16:00- 12/05 02:00	239 (58 -530)	3.9(0.9-8)
Winter Haze Event 5	12/06 09:00- 12/08 10:00	144 (64 -229)	4.6(2.2-8)
Summer Haze Event 1	27/05 12:00 -28/05 13:00	107(62- 163)	6.8(4.5-9)
Summer Haze Event 2	17/06 09:00-18/06 17:00	90.5(60-153.3)	9.3(7-13)

Note: data in parentheses show the range

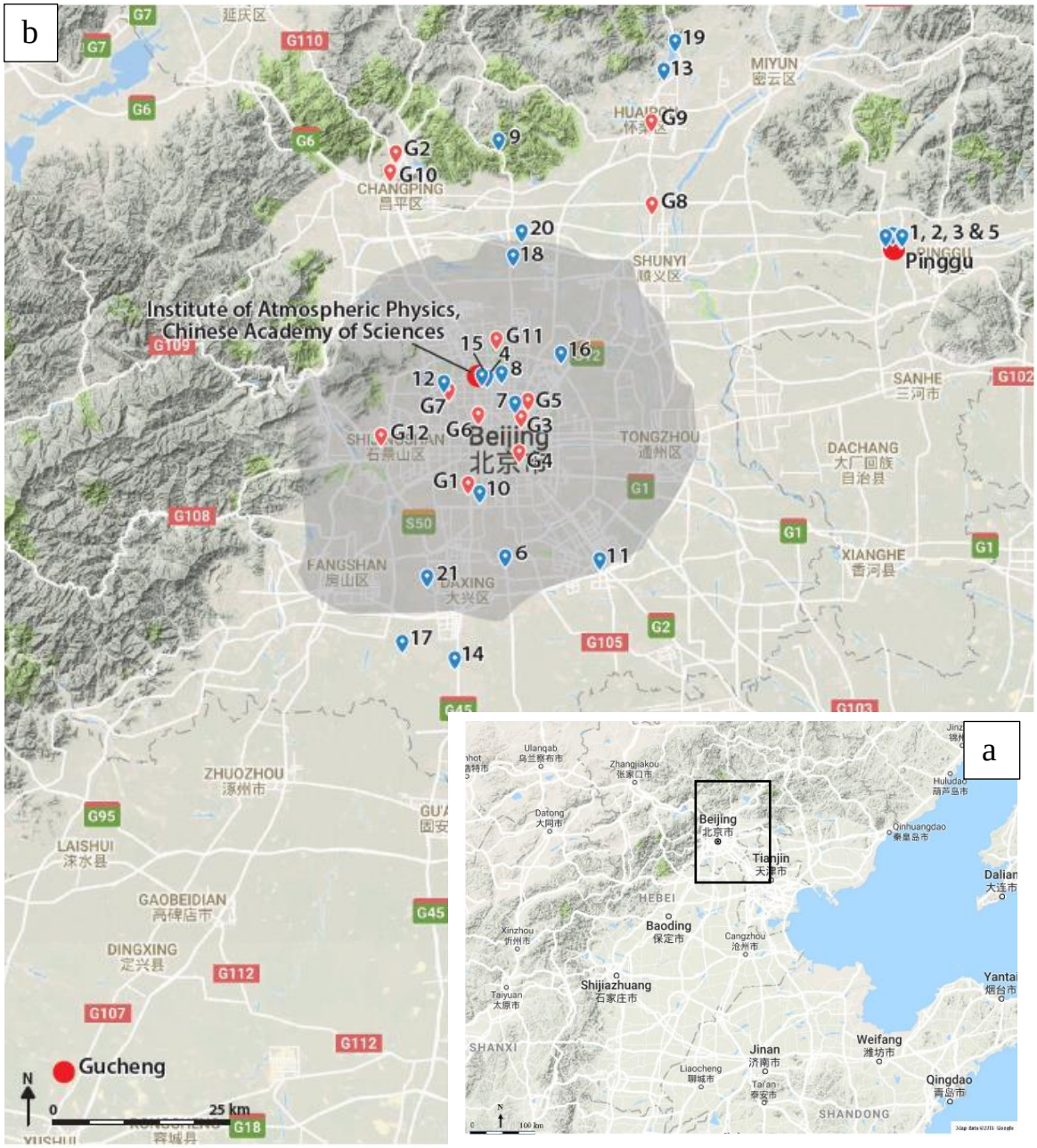

Figure 1: Study area topography (source: googlemap) of Beijing / Tianjing / Hebei region (a) with the rectangle showing enlarged study area; locations of measurement sites (Institute of Atmospheric Physics (IAP)– urban Beijing, Pinggu – rural Beijing; and Gucheng – upwind site in Hebei province), SNAQ box sites (red symbols) and the 12 national air quality monitoring stations (G1 to G12, blue symbols) (b). The shaded area shows the Beijing buildup area. (Source: a and b - Goggle Map topographic background imagery). G1: Wangshouxigong; G2: Dingling (Ming Tombs); G3: Dongsi; G4: Tiantan; G5: Nongzhanguan; G6: Guanyuan; G7: Haidianquwanliu; G8: Shunyxicheng; G9: Huairouzhen; G10: Changpingzhen; G11: Aotizhongxin (Olympic Park); G12: Gucheng. Categories: Urban: G1, G3, G4, G5, G6, G7, G8, G11, G12; Suburban: G9, G10; Rural: G2.

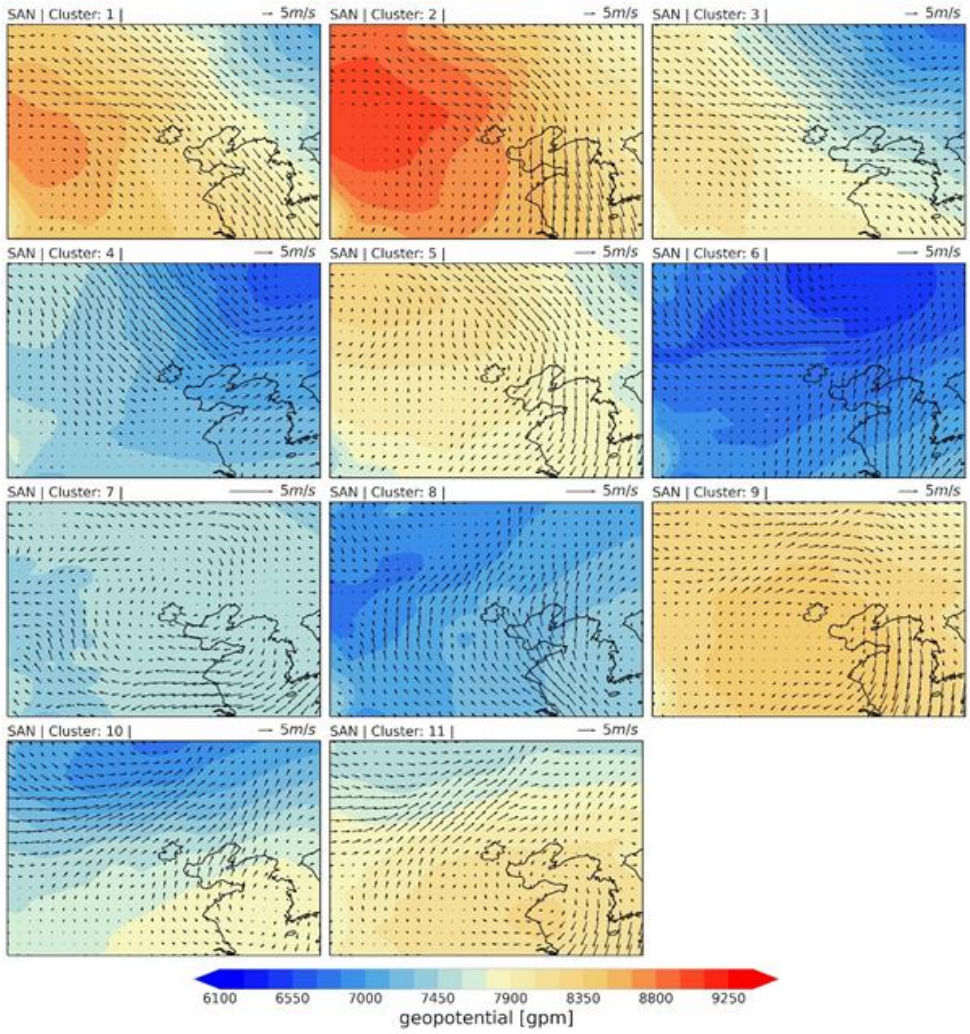

Figure 2: ERA-Interim (1988-2017) average 925 hPa geopotential with 10 m horizontal wind vector for 11 circulation types classified for Beijing (municipal boundary thin solid line) surroundings (103-129° E, 31 - 49° N) determined with the SANDRA method (COST733 class software). Frequency of occurrence is given in cluster caption. For discussion of conditions associated with each CT see Section 4.3.

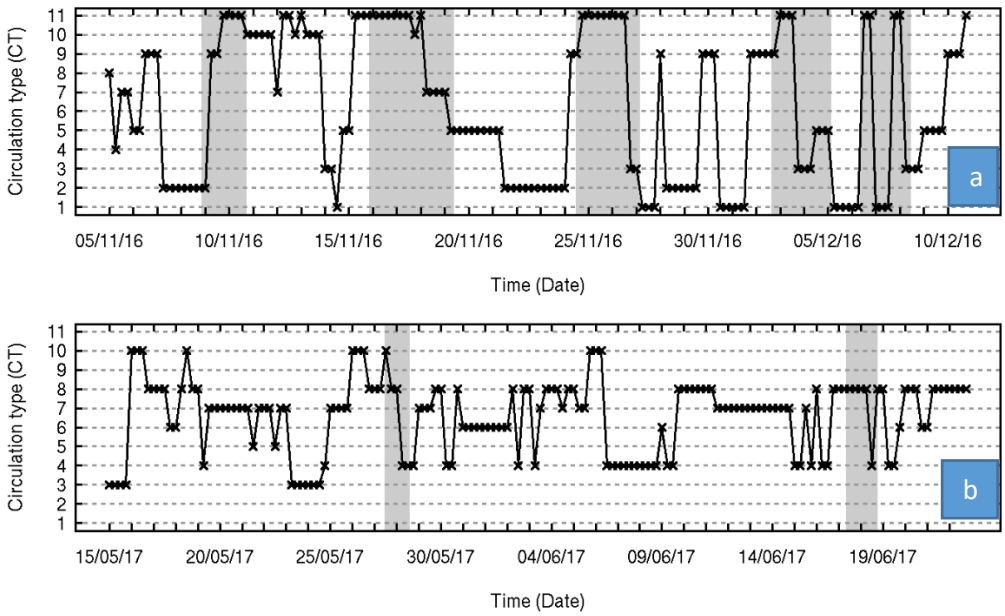

Figure 3: Time series of circulation types (CTs) during the two field campaigns: (a) winter and (b) summer. The 11 CTs are shown in Figure 2. See text for more description. Shading shows the pollution events identified in Section 5 and Figure 5.

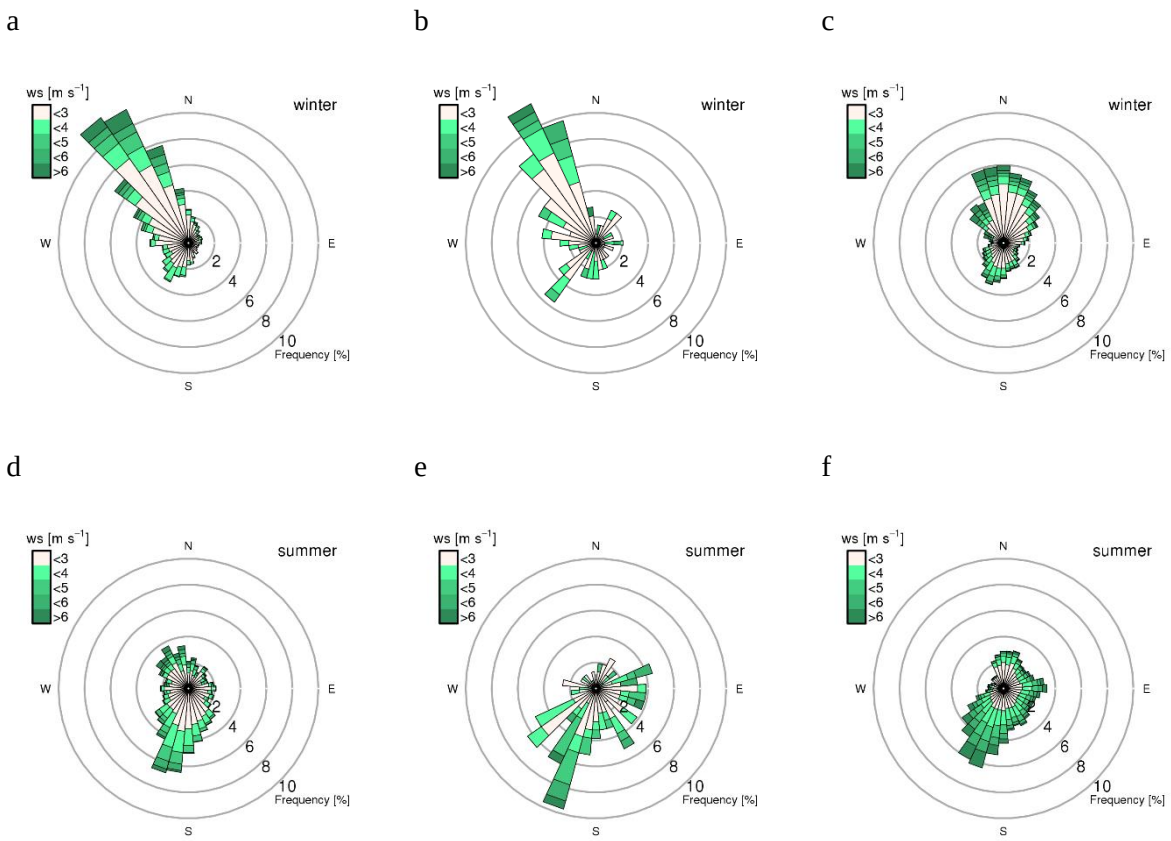

Figure 4: Beijing wind roses: (a, b, d, e) ERA-Interim 10 m horizontal wind (40° N, 116.5° E) and (c, f) sonic anemometer (Table 1) at IAP 320 m agl for (a) 5 November – 10 December in 1988-2017, (d) 15 May – 22 June in 1988-2017, (b, c) 5 November – 10 December 2016, and (e, f) 15 May – 22 June 2017.

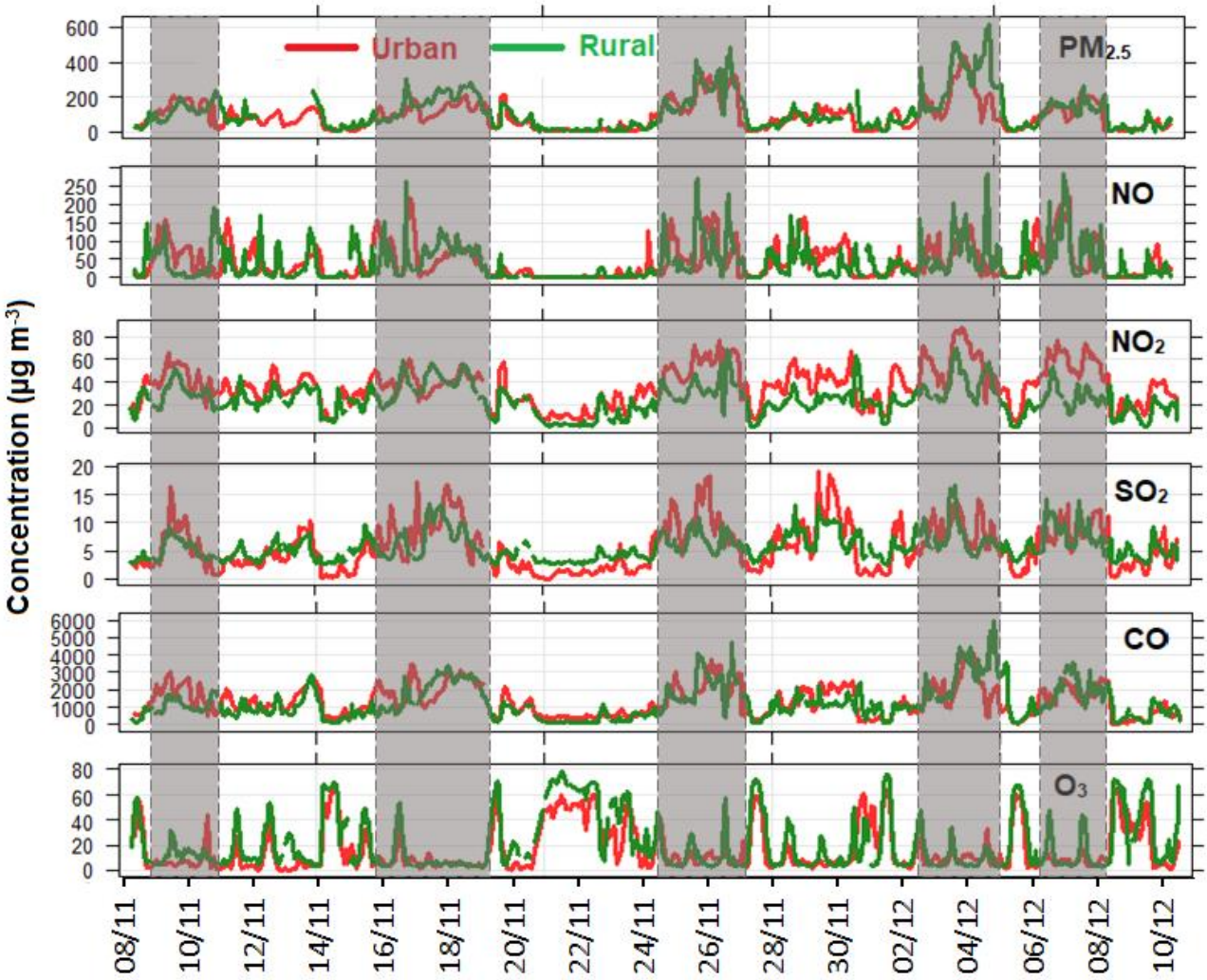

Figure 5: Time-series of air quality variables at the urban and rural sites during the winter campaign; Five haze events are indicated (shading; see also Table 4).

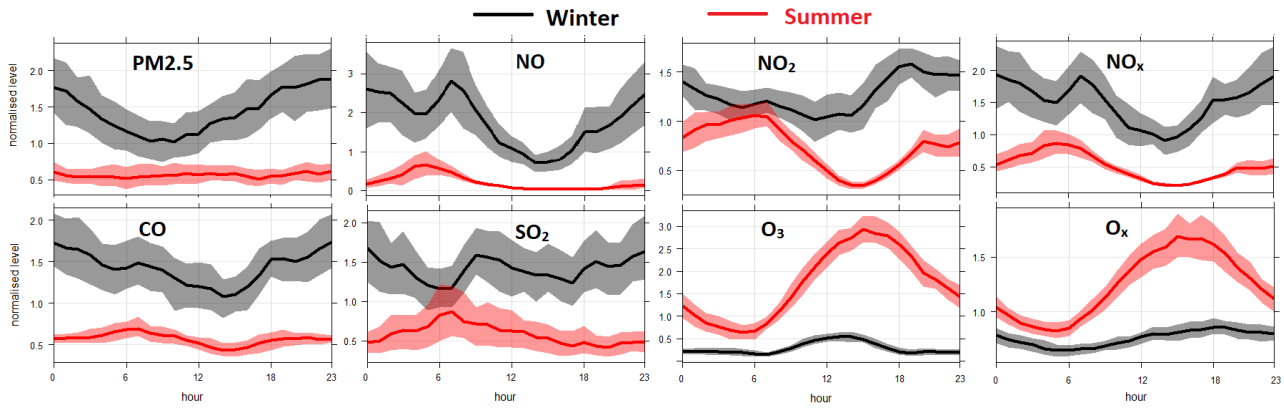

Figure 6: Diurnal patterns of gaseous pollutants normalized by average concentrations at IAP during winter and summer campaigns. Line shows the mean concentrations and shaded area as 95% confidence interval in the difference in mean concentrations.

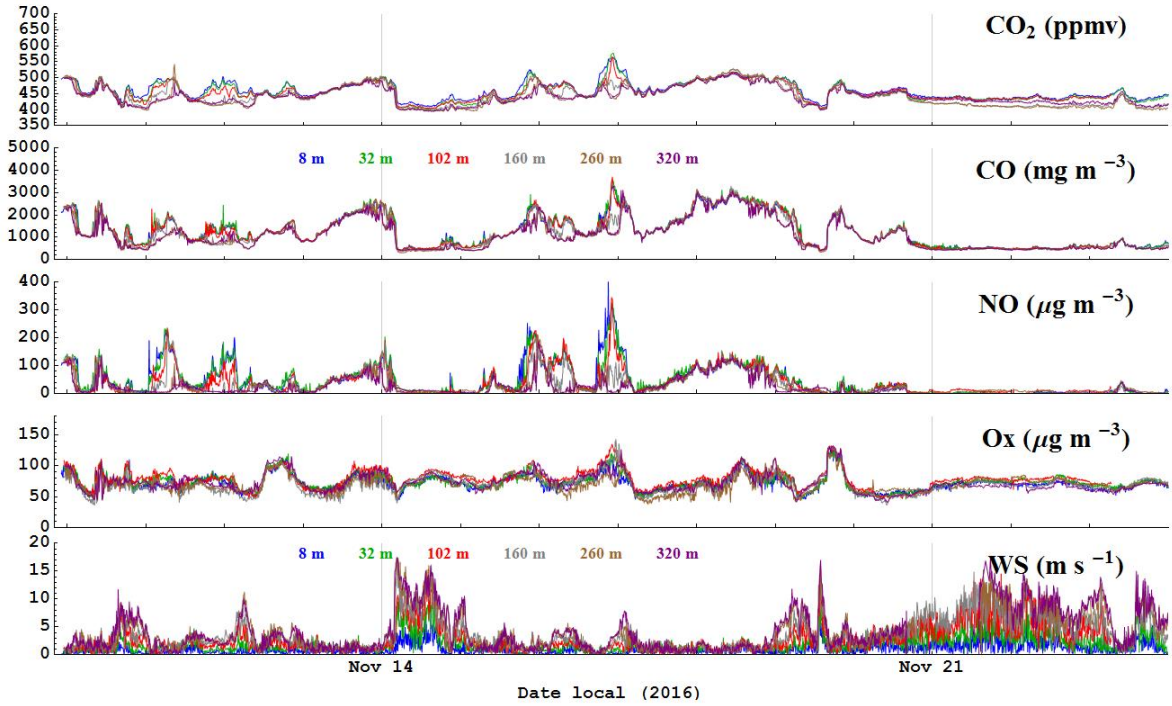

Figure 7: Time series of CO_2, CO, NO, O_x (NO_2+O_3) and wind speed at six heights (colour) measured with SNAQ boxes on the IAP tower during the winter intensive field campaign.

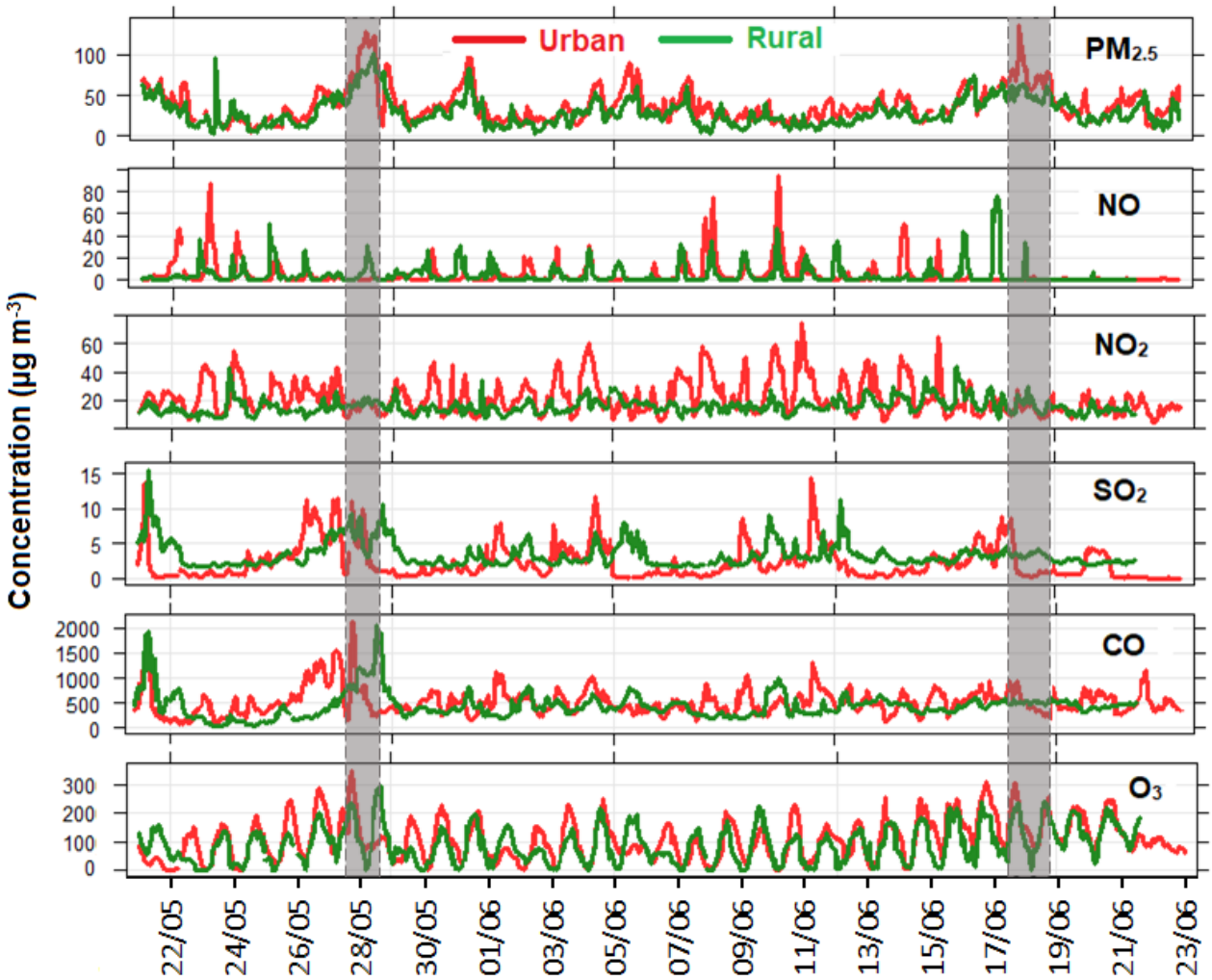

Figure 8: Time-series of air quality variables at the urban and rural sites during the summer campaign. Two minor haze events are indicated (shading).

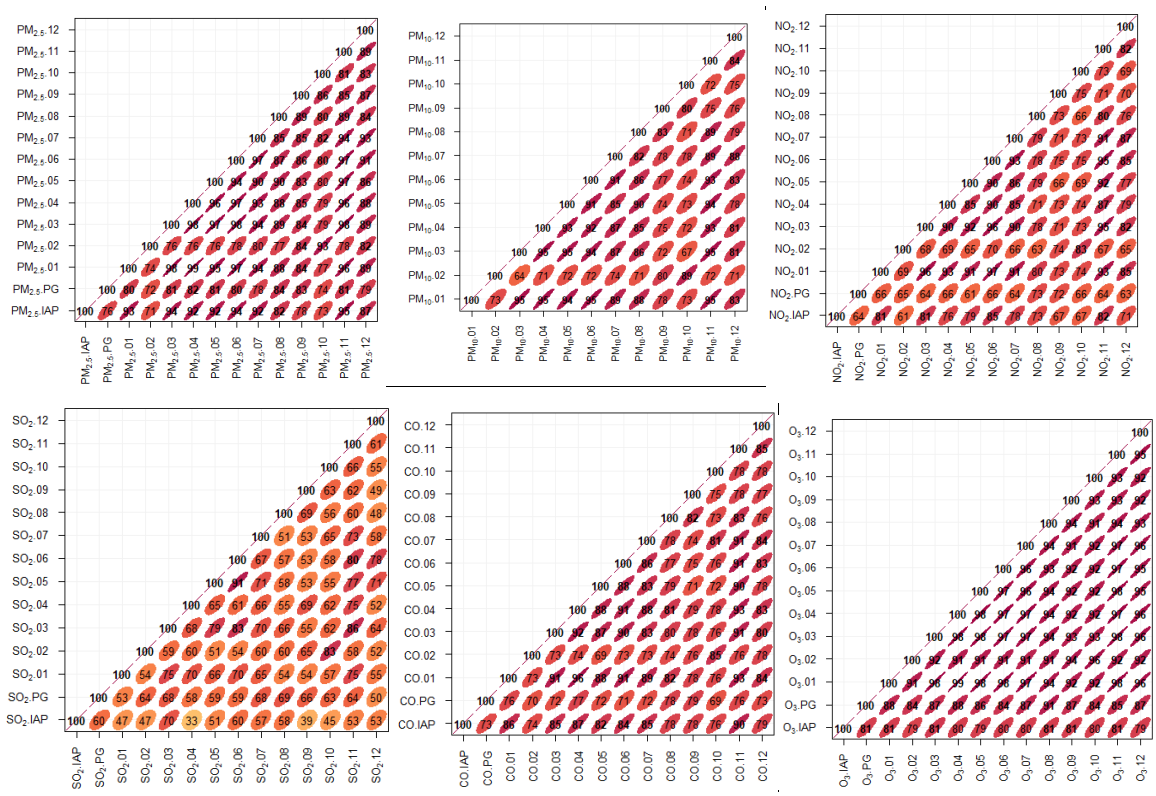

Figure 9: Correlations between the air quality at IAP, PQ and 12 monitoring station around Beijing. Stations G1-G12 (Figure 1(b)) are labelled 01-12, PG = Pinggu.

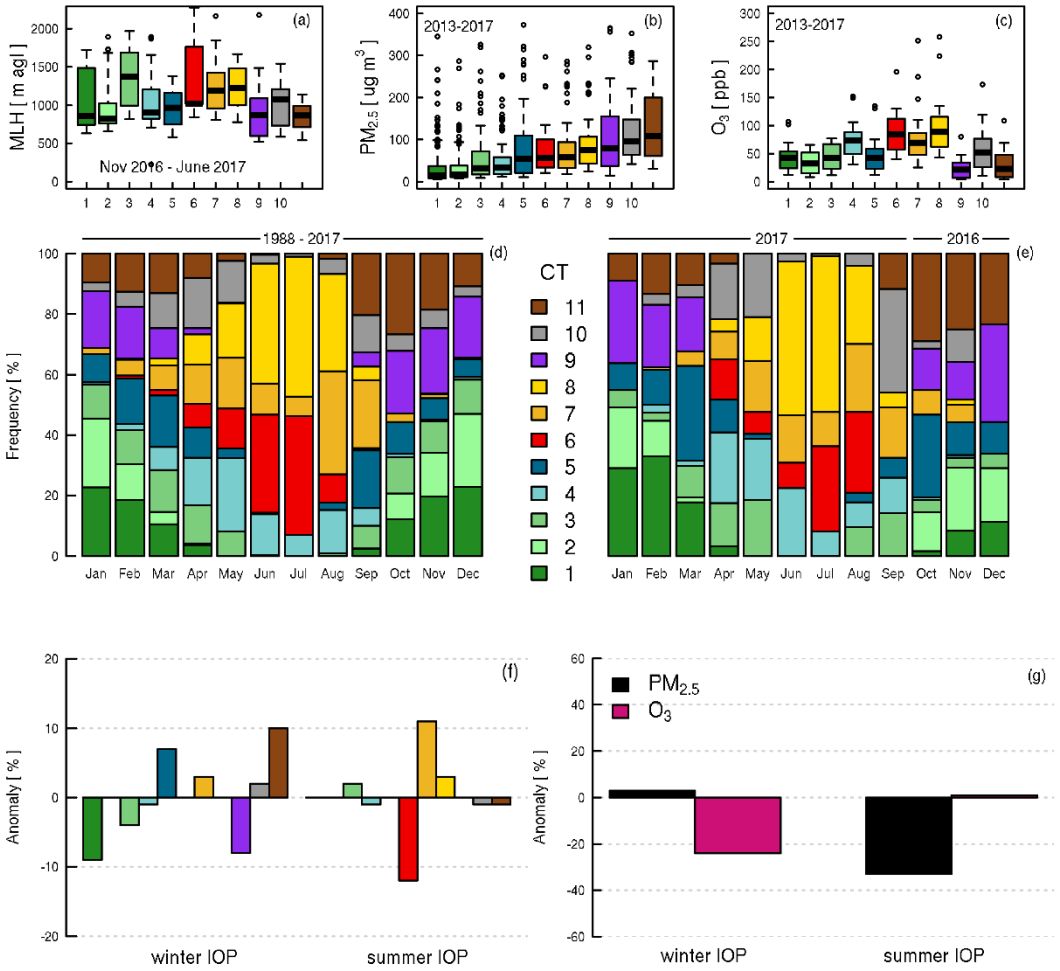

Figure 10: Analysis by circulation type (CT; Sect. 4.3) of: (a) daily maximum mixed layer height (MLH) determined from ALC observations at IAP between November 2016 – June 2017 (analysis method, Kotthaus and Grimmond, 2018b); concentration of (b) $PM_{2.5}$ and (c) O_3 at the Olympic Park (i.e. Aotizhongxin) in 2013-2017 from the national air quality network for different CTs; occurrence of CTs in (d) 1988-2017 and (e) Oct 2016 – Sept 2017; (f) anomaly of CT frequency during the campaigns compared to 5 y (2013-2017) averages; and (g) anomaly of $PM_{2.5}$ and O_3 during the campaigns compared to 5 y (2013-2017) averages. IOP = intensive observation period (i.e., campaign period).

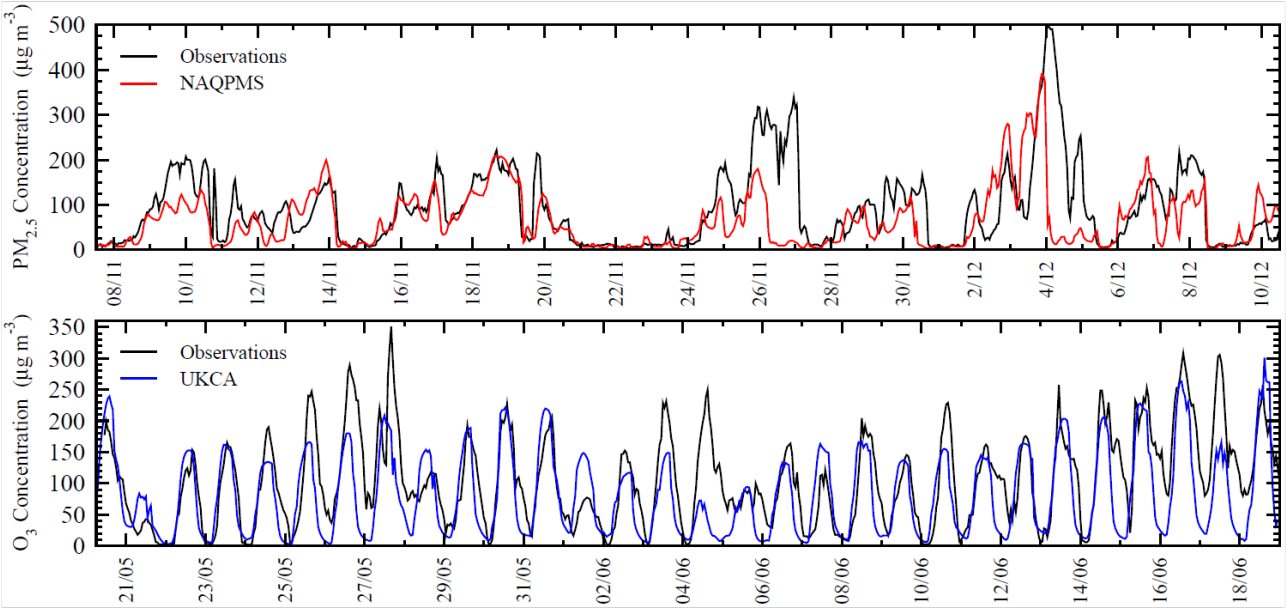

Figure 11: Comparison of observed (at IAP) and modelled pollutant concentrations showing (a) $PM_{2.5}$ concentrations during the winter campaign compared with NAQPMS simulations, and (b) O_3 mixing ratios in summer compared with UKCA simulations.

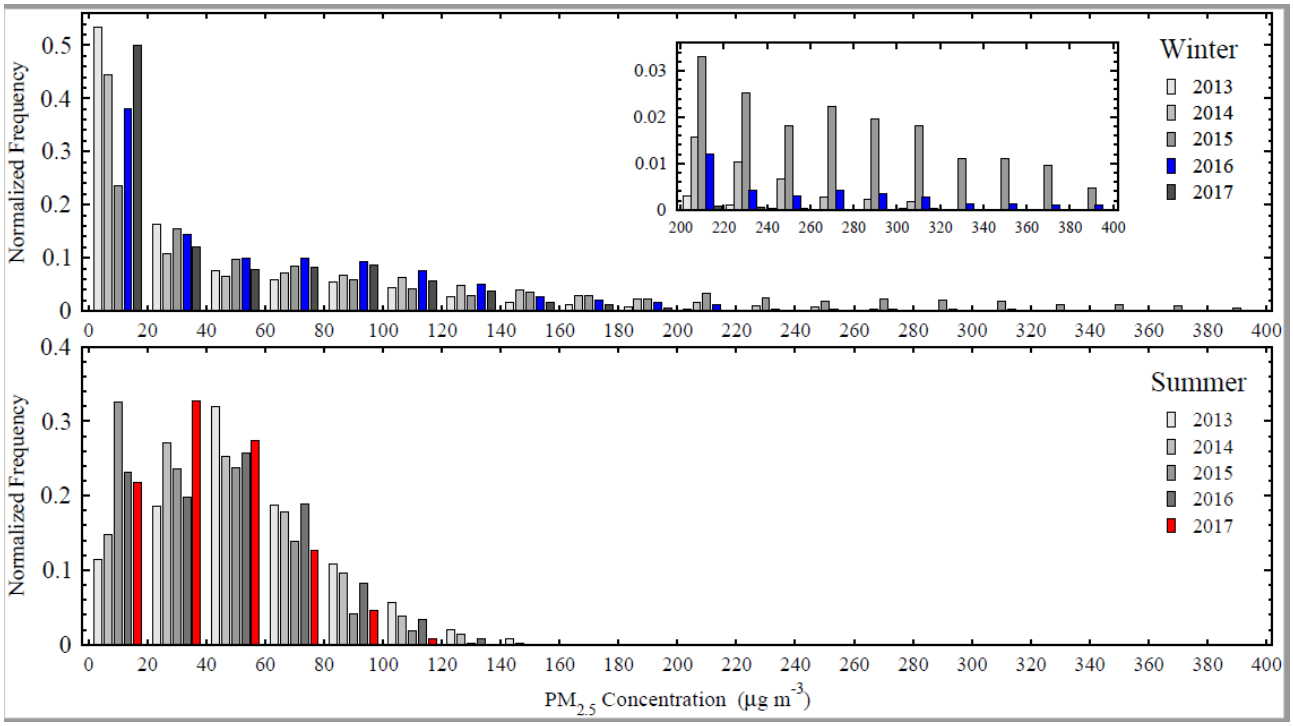

Figure 12: Frequency distribution of $PM_{2.5}$ in Beijing over the winter (top) and summer (bottom) campaign periods from the NAQPMS model compared with those from the same periods over the past five years under the same emission conditions